

Understanding and Managing *C. albicans* Infections

A Thesis

Submitted to the Faculty of Worcester Polytechnic Institute

In partial fulfillment of the requirements for the Degree of

Master of Science

By Catherine G. Harwood

Approved:

Reeta Rao, PhD
Major Advisor
WPI

Robert Gegear, PhD
Committee Member
WPI

Jagan Srinivasan, PhD
Committee Member
WPI

Table of Contents

Table of Figures.....	iii
Abstract.....	iv
Acknowledgements.....	v
Chapter 1: An Introduction to <i>Candida albicans</i>	1
Candida albicans	1
Animal Models	2
Caenorhabditis elegans	2
Ex Vivo Systems	5
In Vitro Systems	6
Available Drugs	8
A Potential Drug: Filastatin	9
Chapter 2: Finding the Target of Filastatin: A Small-Molecule Inhibitor of <i>Candida albicans</i> Adhesion.....	11
Introduction	11
Materials and Methods	12
Adhesion Assay	12
Interaction Assay	12
Biofilm Assay (Glass)	12
Biofilm Assay (Plastic, 96-Well Format).....	13
Results	14
Initial Screen.....	14
Second Screen	15
Atomic Force Microscopy (AFM) Results	18
Interaction Assays: Hemoglobin and Filastatin	20
Discussion	26
Chapter 3: Phenomics Panel on Several Clinical Isolates of <i>Candida albicans</i>	29
Introduction	29
Materials and Methods	32
Growth Conditions for Yeast and Worms.....	32
Egg Preparation	32
Dar Assay	32
Macrophage Assay	33
Adhesion Assay	34
Results	35
In vitro: Adhesion Assay	35
In vivo: Dar Assay	35
In vivo: Survival Assay	37
Ex vivo: Macrophage Assay	40
In vitro: Morphology.....	40
In vitro: Stress Conditions.....	43
Discussion	46
Chapter 4: A Published Review.....	48

Host Pathogen Relations: Exploring Animal Models for Fungal Pathogens	48
1. Introduction.....	48
1.1 Candida	49
1.2 Cryptococcus	50
1.3 Histoplasma.....	50
1.4 Aspergillus	51
2. Animal Models.....	51
2.1 Mus Musculus.....	53
2.2 Zebrafish.....	54
2.3 Drosophila Melanogaster.....	55
2.4 Caenorhabditis Elegans	56
3. Ex Vivo Systems	57
4. In Vitro Systems	58
5. Conclusions	60
Appendix A: Results of the Initial Screen Designed to Find Mutants that Show an Exaggerated Response to Filastatin	61
Appendix B: Results of the Second Screen Designed to Find Targets that Are Blind to the Addition of Filastatin	62
Appendix C: Another View at the Interaction Assay Results.....	65
Appendix D: Summary of Results from Chapter 1	66
Appendix E: Results of the Statistical Analysis on the Survival Assay.....	67
Appendix F: Phenotypic Examination of a Laboratory Tetraploid Strain.....	68
Appendix G: Requirements for Graduation	71

Table of Figures

Figure 1: Model Systems Used to Study Fungal Infections, like <i>C. albicans</i>	4
Figure 2: Stages of Biofilm Formation.....	8
Figure 3: The Original Hypothesis for the Initial Screen That the Targets Would Show an Exaggerated Response.....	15
Figure 4: The Hypothesis for the Second Screen States that the Target Gene Will Show No Response to the Drug.....	16
Figure 5: Iron-Uptake Pathway Working within the Cell.	18
Figure 6: AFM Results for Mutants in the Iron-Uptake Pathway.	19
Figure 7: Adhesion Force Measurements using AFM of Wild Type Strain on Glass and Glass Treated with Filastatin	19
Figure 8: Interaction Assay Results for the Wild Type Strain	21
Figure 9: Wild Type Strain in the Presence of Increasing Concentration of Filastatin (0–50 μ M) and Hemoglobin (0–50 μ M).....	22
Figure 10: Effects of Two Iron Chelators on the Interaction Assay:	23
Figure 11: Biofilm Formation of a Wild Type Strain in Different Media Types.....	24
Figure 12: Biofilm Formation of Wild Type Strain in Different Media Types.....	25
Figure 13: Adhesion of Each of the Clinical Isolate Strain.....	36
Figure 14: Dar Assays Day 4 and 5	37
Figure 15: Survival Comparison between PN1 and PN2	38
Figure 16: Survival Analysis of the FH Series	39
Figure 17: Results of the <i>Ex Vivo</i> Macrophage Assay for a) the PN series and b) the FH series.	41
Figure 18: Attached Cells, Filamenting by Starving Media.....	42
Figure 19: Filamentation Induced by Invasion on YPD Agar Plates of PN Series	42
Figure 20: Attached Cells, Filamenting by Starving Media.....	43
Figure 21: Filamentation Induced by Invasion Assay on YPD Agar Plates of the FH Series	44
Figure 22: Heat Map Indicating Relative Responses of PN Series to Each Stressor	45
Figure 23: Heat Map Showing the Response of the FH Series to Each Stressor	45

Abstract

Candida albicans is an opportunistic fungal pathogen. It is the fourth leading cause of nosocomial infections and can endanger immunocompromised patients. *Candida* has the ability to form biofilms on plastic medical devices, such as catheters and central nervous system shunts. Two clinical isolate series were profiled using a number of phenotyping assays comprising *in vivo*, *ex vivo*, and *in vitro* tests. These tests shed light on host-pathogen relations as well as offer potential information useful in the treatment of these infections. Fluconazole, an antifungal, is the first line of treatment for fungal infections. The incidence of fluconazole-resistant infections is increasing annually, and there are not many other drugs available to treat infections. In 2013, Fazly *et al.* discovered the drug Filastatin, which prevents adhesion and filamentation of *Candida albicans*. In our study, two screens were performed to identify the target of Filastatin. Because there is no complete knockout library for *Candida*, an available, partial knockout library was screened. This library is enriched for transcription factors. We screened for regulators of biological pathways that may be important for adhesion and filamentation in *Candida albicans*, to identify potential Filastatin targets. The iron-uptake pathway was chosen as the focus for the remainder of this study.

Acknowledgements

First, I would like to express my sincere gratitude to my advisor Dr. Reeta Rao for the continuous support of my M.S. study and the research and for her patience, motivation, and enthusiasm. Her guidance was helpful during research and writing of this thesis.

I would like to thank the rest of my thesis committee: Dr. Robert Gegeer and Dr. Jagan Srinivasan, for their encouragement, insightful comments, and tough questions. My sincere thanks also goes to Dr. Claire Benárd, for offering me the summer position in her group and pushing me to work on exciting new projects.

I thank my fellow labmates Toni Delorey and Diego Vargas, as well as past lab members Charu Jain and Luca Issi, for the stimulating discussions, support when experiments (and TA) were not going quite right, and for the fun we have had in the last two years. Additionally, I would like to thank several undergraduates, both past and present. Mike Boyd and Damien Cabral, thank you for your help with the two screens. Rony Noreldin and Jonah Rosch, your work with the AFM was careful and precise, so thank you. Meredith Rioux, I would like to thank you for your help with the *C. elegans* work, and I hope that you will continue it. Finally, Sarah Martin, I would like to thank you for your tireless efforts to keep our lab functioning; additionally, I hope that you learned something when you helped me with the *in vitro* profiling. I certainly could not have done it without you.

Also, I would also like to thank my friends at WPI: Melissa, Chris, Doug, Laura, and others for their support, both emotionally and as scientific sounding boards. Cassie Blanchette, thank you for all that you have taught me and for being my role model as I have completed my graduate work. Last but not the least, I would like to thank my family. To my parents, Carol and Jack Harwood, thank you for supporting me in my pursuit of knowledge, for helping me edit my thesis, for listening to my presentations time and again. Thank you to my rock, Josh, as always, for being there for me.

Thank you

Chapter 1: An Introduction to *Candida albicans*

Candida albicans

Fungi are ubiquitous and can grow in the mucous membranes, intestinal tracts, and on the skin. They are also found in the soil and on plants, trees, and other vegetation. Although not all fungi are pathogenic, some can cause serious disease and pose a significant public health risk. Within the last three decades, fungi have been identified as the leading cause of nosocomial infections (Pfaller, 2007; Prevention, 2014c) especially among immunocompromised patients.

Yeasts that belong to the genus *Candida* can cause both superficial and invasive infections. Superficial infections include oropharyngeal infection or “thrush,” vaginitis (commonly called “yeast infection”), and diaper rash. While superficial infections are often persistent, they are usually not life threatening. However, when *Candida* invades the bloodstream, the infection becomes systemic and is often deadly (Control, 2013; Prevention, 2014b). Fungi in the *Candida* genus have emerged as major human pathogens, becoming the fourth leading cause of bloodstream infections (BSI) in hospitals around the United States, with 7,000–28,000 annual reports of *Candida* specific BSIs (Pfaller, 2007). Some strains, specifically *C. albicans*, are becoming increasingly resistant to conventional antifungal treatments (Pfaller, 2007). For example, in 2013 the United States Center for Disease Control (CDC) reported that fluconazole resistant *Candida albicans* poses a serious threat and is responsible for approximately 3,400 cases annually, including those that are superficial as well as those in the bloodstream (Control, 2013). The lifestyle and virulence strategies used by *C. albicans* are the subject of intense research (Pfaller, 2007). A BSI often begins with a biofilm on medical devices, such as dental implants, catheters, heart valves, bypass grafts, ocular lenses, artificial joints, and central nervous system (CNS) shunts (Prevention, 2014c). In persons whose gastrointestinal tract is heavily colonized by *C. albicans*, it is thought to invade the epithelium in the villi and cross into the bloodstream. The most common non-*albicans* infections seen are caused by the emerging opportunistic pathogens *C. parapsilosis*, *C. tropicalis*, and *C. glabrata*.

Candida parapsilosis is also capable of forming biofilms on catheters, which can lead to systemic infection if the catheter is placed before removing the yeast (Prevention, 2014c). *Candida glabrata*, evolutionarily a distant relative of *C. albicans*, was once considered nonpathogenic (Prevention, 2014c). With the increasing incidence of AIDS and corresponding

rise in the use of immunosuppressive agents, *C. glabrata* infections have also increased as the second most common causative agent of superficial and systemic *Candida* infections. It is often difficult to treat because it is resistant to many azole antifungal agents (Fidel, 1999). *Candida tropicalis* is the fourth most common species of the *Candida* genus (Pfaller, 2007). It is common among patients with hematologic malignancies. It is sensitive to azole drugs and other antifungal agents, which have decreased the incidence of *C. tropicalis* within the United States. However, worldwide, its incidence continues to rise, which makes it a candidate for study (Pfaller, 2007).

Animal Models

Several animal hosts have been used to study fungi that cause these common infections (Figure 1). Each model has its limitations, but can also yield useful information. Therefore, it is crucial that researchers choose an appropriate model best suited to address the experimental hypothesis being tested. The most common host systems are mice, zebrafish larvae, fruit flies, and nematodes. Clinical isolates, from human infections, can provide useful tools, which are often studied using *in vivo*, *ex vivo*, and *in vitro* techniques. Mice are considered the “gold standard” for studying infection because of its direct implication for human systems. The mouse has been used to model oral, vaginal, and systemic infections that have been shown to mimic human infection (Conti, 2009; Fidel, 1996; Takakura, 2003). While this system has many benefits, there are several limitations associated with this study. These limitations include ethical concerns, small sample size, expensive handling, and a laborious knockout process. Therefore in this study, *C. elegans* is the *in vivo* model used to study *C. albicans* infections.

Caenorhabditis elegans

Caenorhabditis elegans has been used extensively as a model system to study various biological phenomena due to many positive aspects including a rapid lifecycle, its completely sequenced genome, genetically identical progeny (due to self-fertilization), and a transparent cuticle that facilitates whole animal microscopy (Stiernagle, 2006). More recently, it has been used as an animal model for the study of infectious disease (Ewbank, 2002; Garsin et al., 2003; Hodgkin, 2000; Jain, 2013). Nematodes are exposed to the infectious agent in their diet, therefore multiplicity of infection is not easily determined (Mylonakis, 2002). Fungi concentrate distally

to the pharyngeal grinder and infected worms show a distended gastrointestinal system (Jain, 2013; Jain et al., 2009; Mylonakis, 2002).

Caenorhabditis elegans has been a host model for many gram-positive and gram-negative bacterial infections such as *Salmonella typhimurium*, *Pseudomonas aeruginosa*, and *Staphylococcus aureus*. Certain long-lived *C. elegans* mutants show immunity to these bacterial infections (Mahajan-Miklos, 1999). Recently, *C. elegans* was used as a host to study fungal diseases, but more importantly, discoveries made in worms recapitulate virulence patterns in mouse and human infection (Mylonakis, 2002). For example, several virulence genes, including protein kinase A (PKA), protein kinase R (PKR), and G-protein alpha (GPA) were first identified in *C. neoformans*, which modulates virulence in *C. elegans* (Mylonakis et al., 2004). These same genes were later shown to be important for *Cryptococcus* infection in mammals (Mylonakis, 2002). Disrupting PKA increases virulence of *C. neoformans* in mice (D'Souza et al., 2001), a phenomenon that was replicated in *C. elegans*.

Infected nematodes show a deformity in the post-anal region (Dieterich et al.), which is visible four- to five-days post-infection (Hodgkin, 2000; Jain, 2013). Other disease markers such as swelling in the vulvar region and intestinal distension have been reported for both fungal and bacterial infections (Hodgkin, 2000; Jain, 2013). Ingestion of yeast can be microscopically monitored over time using fluorescently marked *C. albicans* (Jain, 2013), confirming that accumulation of fungi is the likely cause of intestinal distension.

These disease markers can be used to study the progression of disease, while survival assays provide a quantitative measure of disease and death. As a simple starting model, *C. elegans* is a quick and inexpensive way to study virulence of many fungal species. However, the results often need to be verified in a mammalian system, like mice.

The nematode is a convenient model to study innate immunity, since facets of it are conserved in humans (Jain, 2013; Jain et al., 2009) and host genes can be easily modulated via RNAi (Kim and Rossi, 2008). Furthermore, infections do not require handling of animals, and therefore, can be performed in a high throughput fashion. Another advantage is that worms can be frozen (indefinitely) and thus do not require maintenance of live cultures.

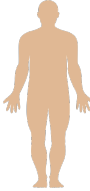






		BENEFITS	LIMITATIONS	
ANIMAL MODELS		 Human	Clinical samples from patients with active infection Hypothesis free experiments	Purifying selection when cultured in laboratory IRB needed Not experimental host Hypothesis generated need to be tested in model host
	Vertebrate	 Mouse	Several modes of infection BSI Oral Vaginal Mammalian immune system	Expensive Handling of individual animals Testing hypothesis is not trivial Overwhelm the immune system Small sample size
		 Zebrafish	Vertebrate model Primitive phagocytes present Experimentally tractable	Maintain live animals Handling of individual animals
	Invertebrate	 Fruit fly	Primitive phagocytes present Experimentally tractable	Maintain live animals Handling of individual animals Dosage not controlled for oral feeding Wild type fly resistant to infection
		 Nematode	High-throughput applications Experimentally tractable Large sample size Innate immune pathways conserved Can be frozen indefinitely	No phagocytes
	OTHER MODELS	Ex vivo	 Cell culture	Primary phagocytes Immortalized phagocytes High-throughput screening
In vitro		 No host	Phenotypic characterization Morphology Drug sensitivity Biofilm formation Competitive fitness	Not physiological

Figure 1: Model Systems Used to Study Fungal Infections, like *C. albicans*

***Ex Vivo* Systems**

Ex vivo systems for studying fungal infections include phagocytes in culture and tissue explants, as shown in Figure 1. Phagocytes are our primary defense against fungal pathogens. Macrophages and neutrophils play a central role in antifungal immunity by ingesting and killing pathogens (Lo, 1997; Lorenz and Fink, 2001; Rubin-Bejerano et al., 2003; Wheeler and Fink, 2006). They are also responsible for initiating adaptive immune responses.

Cultured macrophages can include both primary and immortalized cells. Immortalized cell lines such as the RAW264.7 and J774 are robust and can withstand harsh treatments to remove these adherent cells from surfaces, such as trypsinization and scraping, while still proliferating. Immortalized macrophages have been instrumental in uncovering aspects of *Candida* virulence such as hyphae formation, extracellular lipase, and proteinase production (Németh, 2013). However, the multiple passages and harsh growth and handling conditions of immortalized macrophages specifically select them to be more robust at the expense of other properties that might be important for immunity. Therefore, primary macrophages are considered better for studying immunity than immortalized macrophages even though they are more difficult to extract and maintain (Németh, 2013).

Németh and others (2013) infected both immortalized murine macrophage and primary human macrophage hosts with *Candida parapsilosis* in the paper “Characterization of Virulence Properties in the *C. parapsilosis Sensu Lato* Species” (Németh, 2013). The fungi exhibited varying degrees of virulence when exposed to each type of macrophage (Németh, 2013). *C. parapsilosis* exhibited the highest resistance to killing by primary human macrophages, compared to *C. orthopsilosis* and *C. metapsilosis*. However, this difference was not reflected in the murine virulence model. In spite of these differences, cultured cell lines are useful and can complement live, whole-animal studies.

Transcriptional profiling of *C. albicans* within phagosomes has been performed (Thewes, 2007). Strains have been shown to quickly adapt and alter their transcriptional profile in many circumstances related to infection, such as response to stress, iron deprivation, and interaction with macrophages. In order to understand *Candida* infection, Thewes and others (2007) used *in vivo* and *ex vivo* techniques to understand the genes associated with infection in parenchymal organs (e.g., the liver). An *ex vivo* tissue explant of porcine liver-infected tissue was shown to mimic murine model of *in vivo* infection. *Candida albicans* was directly injected into both mice

and pig livers. *Ex vivo* tissue explants from both exhibited a similar extent of deep-tissue invasion (Thewes, 2007). Excised murine vaginal mucosal tissue is also used as a substrate to study vaginal infections (Harriott et al., 2010). These *ex vivo* systems provide a simple and rapid method for optimizing conditions prior to *in vivo* assays (Fazly et al., 2013).

***In Vitro* Systems**

Viewing a fungal phenotype on an agar plate is a “host-free” method to study fungal virulence. For example, *C. albicans* mutants such as *efg1*^{-/-} and *cph1*^{-/-} showed reduced hyphal growth on agar media, and the double knockout *efg1*^{-/-} *cph1*^{-/-} does not form hyphae under most *in vitro* conditions. This double knockout mutant was later shown to be avirulent in a murine model, which linked hyphal growth and virulence (Lo, 1997). Since then, many mutants with defects in dimorphic transition have been shown to be attenuated in virulence. This *efg1*^{-/-} *cph1*^{-/-} double mutant has been used extensively to validate other host models (Brothers, 2011; Jain, 2013).

Chemical sensitivity *in vitro* can be used as a proxy for pathways that are important *in vivo*. Fungal response to important aspects of the human innate immune system such as reactive oxygen species can be mimicked *in vitro* using menadione and hydrogen peroxide (Homann, 2009). Cell wall stressors such as sodium dodecyl sulfate (SDS), caffeine, and calcofluor (Homann, 2009) have been used *in vitro* to study the effects on the cell wall. Since human cells do not possess cell walls, they are good targets for drugs, like capsosungin (Homann, 2009). Other drug sensitivity assays can be modeled *in vitro* by plating fungi on drug-infused plates (Homann, 2009). The role of metals can be mimicked *in vitro* by using scavengers or chelators *in vitro*. For example, the *C. albicans* transcription factor Hap43 is activated by iron deficiency *in vivo* (Hsu et al., 2011) and is also required for growth upon iron-deprivation *in vitro* (Baek et al., 2008; Homann, 2009; Hsu et al., 2011). Hap43 also regulates virulence, and mice infected with *hap43*^{-/-} strains showed attenuated virulence (Baek et al., 2008). The pathways regulating iron homeostasis are complicated, but *in vitro* techniques may be used to fine tune regulatory networks.

In vitro models can also be used to study reconstituted epithelial cells in order to model human infection (Figure 1). The role of certain virulence-related genes in fungal infection can first be modeled *in vitro* on reconstituted epithelial cells before using more expensive *in vivo*

models. For example, the secreted aspartyl proteinases (SAP) of *C. albicans* have been linked to virulence in mucosal infection in clinical isolates of patients with chronic vaginitis (Schaller, 2003). This family of 10 enzymes was first studied using reconstituted vaginal epithelial cells in order to link them to epithelial damage that occurs during disease. The 10 *SAP* genes are differentially expressed during infection. Specifically, *SAP1*, *SAP6*, *SAP9*, and *SAP10* showed a stronger signal in conjunction with mucosal lesions (Schaller, 2003). These *SAP* genes showed strong signals in both *in vitro* models as well as *in vivo* samples from patients with vaginal infections. These lesions showed severe damage in the epithelial cells including: edema, vacuolization, and detachment of keratinocytes. Differential SAP expression has also been linked to “thrush” infections (Schaller, 2003). Despite this, they are not identical to those present in vaginal infections (Schaller, 2003).

Biofilm formation is a virulence determinant that is well suited to study in a host-free environment. Biofilms are typically made up of multiple microbial communities that stick to each other and also abiotic surfaces (Hogan et al., 2004; O'Toole et al., 2000). The microbes secrete extracellular materials (Chandra, 2001) and are important in the context of infection because they are drug resistant. For example, *C. albicans* is thought to gain access to the bloodstream via plastic devices such as central lines, catheters, or other implanted devices. The mortality rate for patients with catheter-related BSI is approximately 41 percent (Chandra, 2001). Biofilm associated cells have shown resistance to antimicrobial therapies as well as phagocytes and antibodies (Li et al., 2012).

As shown in Figure 2, formation of biofilm proceeds in four stages. During the first stage, the fungal communities attach to the surface, grow, and aggregate. The second stage is thought of as irreversible attachment. The third is characterized by filamentation of the yeast cells. Finally, in the last stage an extracellular matrix, a predominantly noncellular material, covers fungal microcolonies and is secreted into the milieu (Chandra, 2001). Biofilm formation plays a role in resistance to antifungal drugs, which can be explained by several factors. These factors include the effect of the biofilm matrix on penetration of the drugs, the decreased growth rate and nutrient limitation characterized by the biofilm, the expression of the resistance genes, and the presence of “persister” cells (Douglas, 2003).

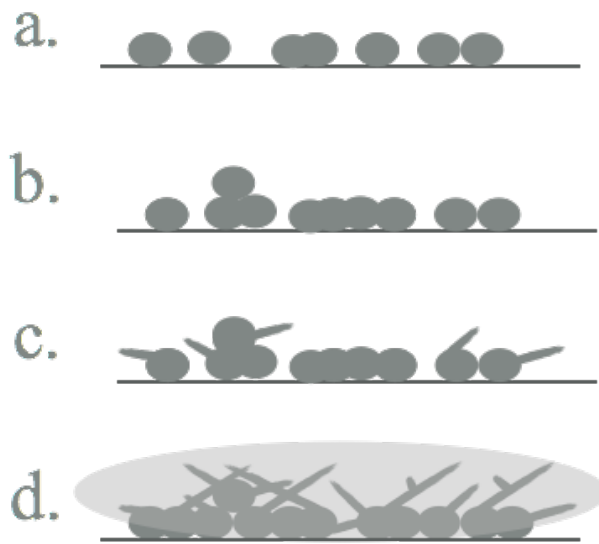


Figure 2: Stages of Biofilm Formation. The first stage (a) initial attachment takes between 0 and 4 hours; the second, (b) irreversible attachment, between 4 and 10; filamentation (c) after 10 hours; the last stage (d) biofilm formation, takes more than 24 hours (Joseph Heitman, 2006a).

In vitro systems are extensively used to study fungal virulence to get mechanistic clues, but often have to be validated in an animal model to account for the complex biology in the host environment. Each of these systems is used to study *Candida* with the hope of finding better methods to treat infections.

Available Drugs

Several antifungals are available on the market to treat *C. albicans* infections. There are four types of available antifungal drugs: polyenes, nucleic acid synthesis inhibitors, echinocandins, and ergosterol biosynthesis inhibitors (EBI). The most popular are the azole drugs, but the known mechanism of each will be discussed briefly.

Polyenes, like amphotericin B (AmB) and nystatin, target ergosterol in fungal membranes. They work by binding to ergosterol and creating pores to allow molecules to diffuse across the membrane, which results in cell death. AmB is used for severe systemic infections, especially when rapid response is needed. However, like many drugs, in high doses, AmB is associated with nephrotoxicity (Joseph Heitman, 2006b).

Fungi and plants are able to convert 5-Flucytosine (5FC), the available nucleic acid inhibitor, into 5-fluorouracil, which is then incorporated into the DNA and RNA. Mammals do not

possess the cytosine deaminase that performs this conversion, which makes this drug fungal specific. However, there is a high incidence of resistance to this drug (Sheikh et al., 2013).

Echinocandins are the newest drugs available to treat fungal infections. They work to inhibit β -1,3-glucan synthase, which is responsible for the production of the glucan component of the cell wall. There are several strains developing resistance to this class of drugs as well (Beyda et al., 2012).

Azoles are the most popular EBI antifungal agents, which work to inhibit the synthesis of ergosterol. When fungi lack ergosterol in the plasma membrane, this results in the loss of the plasma membrane function and fluidity, which inhibits cell growth (Taff et al., 2012). Fluconazole, an azole drug, is usually the first line of defense for treatment. Resistance is also developing to this popular drug. There are roughly 3,400 Fluconazole-resistant *Candida albicans* infections annually. Thus there is a demand for new drugs.

Biofilm formation can provide up to 1,000-fold more resistance to antifungal drugs, even without the presence of genetic markers that are known to provide resistance (Ramage et al., 2005). Potential drugs could therefore 1) target the components of the biofilm (Taff et al., 2012) or 2) prevent biofilm formation (Fazly et al., 2013).

A Potential Drug: Filastatin

In 2013, the Rao and Kaufman labs performed a screen of the Chembridge Chemical library of 30,000 small-molecule compounds to identify new compounds that prevent *Candida albicans* adhesion to plastics. Adhesion is the first step in biofilm formation (Figure 2). In this screen, the mutant *edt1* $-/-$ was used as a positive control for poor adhesion because it lacks a cell wall adhesion protein (Fazly et al., 2013). The primary screen found 400 compounds (1.3 percent) that prevented adhesion by more than 75 percent to the plastics. A second screen was performed on the 400 compounds identified from the primary screen in order to rule out phenotypes potentially caused by an artifact of the assay used in the first screen. Twenty-six compounds were identified from this screen. These 26 compounds were tested *in vivo* for toxicity and dose dependence (Fazly et al., 2013). In addition, structural analysis was performed. The initial concentration tested was 50 μ M, and several of the drugs were ineffective upon reducing the concentration to 25 μ M. One compound, Filastatin, was identified because it prevented adhesion

and filamentation, was non-toxic, and performed well at lower concentrations (Fazly et al., 2013).

In addition to preventing adhesion to plastics, Filastatin also prevents attachment of *Candida* to human epithelial cells, which may limit virulence. Filastatin also prevents adhesion of other *Candida* species: *dublinsiensis*, *tropicalis*, and *parapsilosis*. It has been shown to exhibit antifungal activity in *C. elegans* as well (Fazly et al., 2013). The mechanism of the pathway is not yet known and must be identified before it can be used in a clinical setting. One goal of this thesis project was to perform a screen of a *C. albicans* mutant library to find potential targets and target pathways of the drug Filastatin. Additionally, once these pathways were identified, several experiments were performed to elucidate Filastatin's role within it. Clinically relevant strains, from two patients, were tested to make connections between virulence and adhesion. In addition, the strains were tested in *C. elegans* for virulence and using the *ex vivo* model, murine macrophages. An *in vitro* profile was created for each of the strains. Finally, a synthesis of host-pathogen relations and the model systems used to study a wide range of fungal pathogens was created to further this field of study.

Chapter 2: Finding the Target of Filastatin: A Small-Molecule Inhibitor of *Candida albicans* Adhesion

Introduction

Filastatin, a small-molecule that prevents adhesion, was discovered in 2013 using a screen of 30,000 compounds from a small-molecule library (Fazly et al., 2013). Through toxicity, dose dependence, and structural analysis, Filastatin was determined to have potential implications for future clinical use to prevent *C. albicans* biofilm formation. Before Filastatin can be used at the bedside, the mechanism of action must be identified. In order to identify the target of a drug, normally, a screen of a total knockout library would be preformed. However, there is no total knockout library—instead, an available partial library was screened (Noble et al., 2010). Using the same adhesion assay performed to discover the drug, two screens were performed on this available knockout library to look for potential targets and pathways.

The iron uptake pathway was identified using this screen. This pathway plays a role in virulence as well as adhesion. *Candida albicans* is able to utilize hemoglobin, which is the largest source of iron in the host. Rbt5 is the receptor for acquiring hemoglobin from the environment. It dissociates heme from the globin, and a heme oxygenase, Hmx1, degrades hemoglobin to α -biliverdin (Butler et al., 2009). Finally, the cell takes up the released iron into the cytoplasm (Kornitzer, 2009).

There are two sources of iron that *Candida* can utilize, Fe^{2+} or Fe^{3+} . Hemoglobin is a 64 kDa globular protein. Each of the heme groups binds an iron ion in the ferrous form (Fe^{2+}); oxidation of the iron yields the ferric form (Fe^{3+}). About 30 percent of the iron available in the human body is sequestered in ferritin, as Fe^{3+} . *C. albicans* is also capable of utilizing ferritin as an iron source as well as the ferrous iron from hemoglobin. This method is dependent on cell surface adhesion and the protein Als3. An *als3* mutant has been shown to have reduced ability to invade epithelial cells and is unable to bind ferritin (Kornitzer, 2009), indicating it is vital for this type of iron uptake.

Filastatin could be playing a role in the iron-uptake pathway in several ways: 1) by interfering with the cell's ability to use hemoglobin, 2) by sequestering ferrous or ferric iron and preventing the cell from utilizing it, or 3) by interfering with mechanisms downstream to prevent adhesion.

Materials and Methods

Adhesion Assay

For the target screen, single colonies were picked and inoculated into five milliliter cultures of Synthetic Complete Media (SC) (Sherman, 1991) + 0.15 percent glucose media and grown overnight in a rotating wheel. The optical density (OD) of the cultures was then measured at OD_{600nm}. Cultures were spun down and re-suspended in fresh SC + 0.15 percent glucose to a final concentration of 0.5 OD/mL. *C. albicans* strains, 200 μ L at 0.5 OD/mL, were pipetted onto 96-well flat-bottom polystyrene plates. Filastatin or DMSO was added to cultures at appropriate concentrations, never exceeding one percent DMSO. Plates were covered with aluminum foil and incubated at 37°C for four hours. After four hours of incubation, plates were decanted, and 40 μ L of 0.5 percent crystal violet (CV) stain was added to each well. The plates were covered and left at room temperature to incubate for 45 minutes. Plates were then decanted and washed by submersion 10 times in an ice bucket filled with dH₂O, changing the water every five washes. Plates were tapped onto a paper towel to remove residual dH₂O, and 200 μ L of 75 percent MeOH was added to each plate and incubated at room temperature for 30 minutes. The plates were then read at 590 nM to detect relative absorbance.

Interaction Assay

The adhesion assay was performed as outlined above using the wild type strain from the mutant knockout library (Noble et al., 2010). Filastatin and hemoglobin were added to the cultures at the outlined concentrations. Ferrozine was added in 1 mM concentration (Weissman and Kornitzer, 2004) to the SC media prior to resuspending the *C. albicans* and performing the adhesion assay.

Biofilm Assay (Glass)

A culture of wild type *Candida* from the knockout library (Noble et al., 2010) was grown in YPD media (Sherman, 1991) overnight at 30°C. This strain was resuspended at 0.01 OD/mL in five milliliters of SC media (Sherman, 1991), containing the appropriate concentrations of

Ferrozine, Filastatin, and hemoglobin. Pictures were taken after 24 hours, and the biofilms inspected visually.

Biofilm Assay (Plastic, 96-Well Format)

The wild type strain from the knockout library (Noble et al., 2010) was grown overnight in YPD media and resuspended to a final concentration of 0.01 OD/mL in SC media containing + 0.15 percent glucose. In a 96-well plate, 200 μ L of the *Candida* was dispensed. Appropriate concentrations of the Ferrozine, Filastatin, and hemoglobin were added to the wells. The plates were incubated for 20 to 24 hours and then decanted. The CV stain was added and the rest of the Adhesion Assay protocol followed.

Results

Two screens were carried out in order to find the target of Filastatin. From these screens, two major pathways were identified: filamentation and iron-uptake. We chose to focus our attention on the iron-uptake pathway because it has already been shown that Filastatin prevents filamentation.

Initial Screen

For the original hypothesis, shown in Figure 3, it was postulated that the mutants that would act as the target for the drug would behave like wild type without the drug. The wild type strain adheres to plastics, and thus mutants within two standard deviations of wild type adhesion would be considered. From these mutants, in the presence of the drug, there would be an exaggerated (more than a 25 percent) change in adhesion. This threshold, 25 percent, was set by the lab upon viewing the data as a whole. The wild type showed between 10 and 25 percent reduction in adhesion, regularly, when the drug was added. Therefore, the exaggerated response, compared to wild type, could indicate that there was either a more than 25 percent increase *or* decrease in adhesion.

A summary of the results from this screen is shown in Table 1. From the initial screen, 233 mutants were found, which is about 35 percent of the library and about four percent of the genome. There were two mutants, *fad3* and *orf19.1239*, that adhered more than wild type in the presence of the drug. In the presence of the drug, the rest, 231 mutants, adhered less than the wild type; the list of these genes can be found in Table 1 of Appendix A.

The number of mutants found from this screen was a large part of the library, about 35 percent. Despite the fact that it is only four percent of the genome, the coverage that the library provides is only about 12 percent of the genome, meaning it would likely be significantly more if the coverage of the library was greater. Gene Ontology (GO) term analysis was used to classify genes into relevant pathways. The results showed that many of the genes were involved in filamentous growth, cellular response to stimuli, and response to nutrient levels. The fact that several of the genes were involved in filamentous growth validates this screen because it is known that Filastatin prevents filamentation. The number of genes prevented further useful analysis though, so a second, more stringent screen was designed.

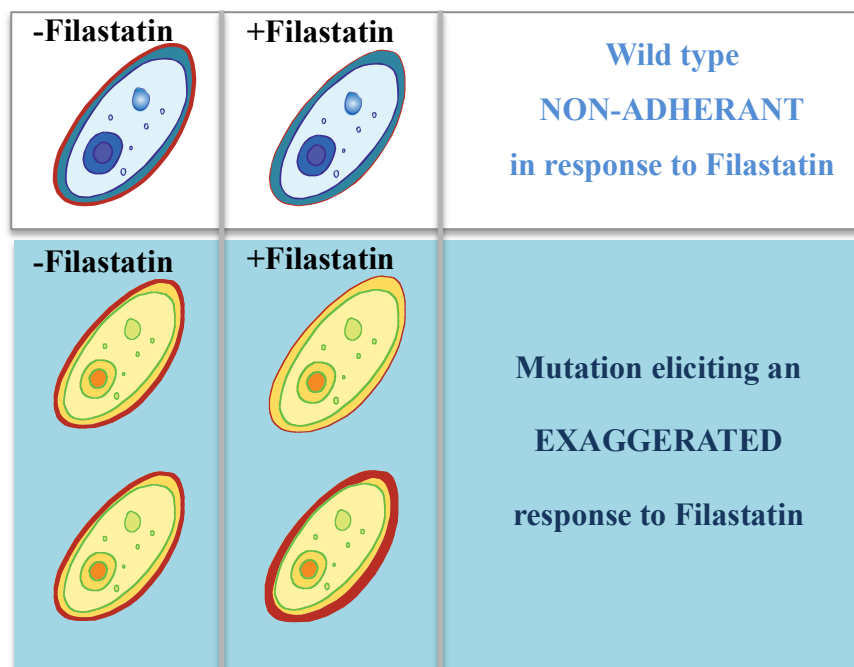


Figure 3: The Original Hypothesis for the Initial Screen—Targets Would Show an Exaggerated Response to Filastatin. Mutants (shown as yellow cells) show a similar level of adhesion to plastic (shown in red) without the drug, but in the presence of the drug, they show an exaggerated response. (Figure based on an original by R. P. Rao (Rao, 2015c))

Table 1: Summary of Results from Initial Receptor Screen. There are a significant number of mutants that adhere less than wild type (WT).

Summary of Results: Initial Screen			
Mutants	Number of Mutants	Percent of Library	Percent of Genome
Adhering more, with drug, than WT	2	0.3%	0.03%
Adhering less, with drug, than WT	231	34.3%	3.85%

Second Screen

Because of the high number of mutants and over-representation of non-descript pathways from the first screen, a second screen was performed to narrow down the results. The new hypothesis, shown in Figure 4, stated that the target mutants would not be affected by the drug's presence. The mutants were significantly (at least two standard deviations) different from the wild type without the drug. When the drug was added, these targets showed a change of less than 10 percent.

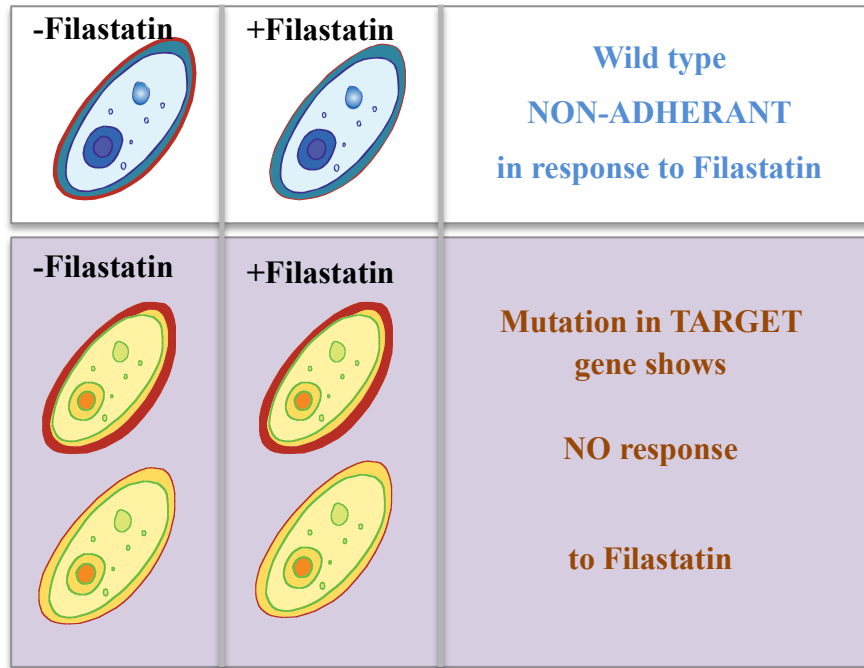


Figure 4: The Hypothesis for the Second Screen States—Target Gene Will Show No Response to the Drug. Mutant cells, shown in yellow, show a significant difference in adhesion (shown in red) without the drug to wild type. However, when the drug was added, the mutants showed no change in adhesion level. (Based on a figure produced by R.P. Rao (Rao, 2015a))

From this screen, 43 mutants were identified. A summary of the results is shown in Table 2. The mutants were screened initially for a different level of adhesion, by at least two standard deviations, from the wild type with no drug. These mutants were then screened with the drug, looking for a mutant that showed less than a 10 percent change in adhesion. There were 28 mutants that showed an increase in adhesion compared to wild type with no drug, and 15 mutants that showed a decrease in adhesion compared to wild type. These mutants showed less than a 10 percent change in adhesion when the drug was added. It was expected that the genes represented in this list would code for a protein that would normally act with Filastatin; thus when the protein was missing, the mutants would be blind to the addition of the drug.

Table 2: Summary of Results from Second Target Screen

Summary of Results			
Mutant	Number of Mutants	Percent of Library	Percent of Genome
Mutants that adhere LESS than WT with no Filastatin	28	4.1%	0.4%
Mutants that adhere MORE than WT with no Filastatin	15	2.2%	0.2%

The full list of mutants found from this screen can be found in Tables 1 and 2 of Appendix B. GO term analysis was used to classify genes into relevant pathways. Two pathways were over-represented. The first were genes that regulate adhesion and biofilm formation. This is not surprising because the screen was designed to find targets related to adhesion and filamentation. The second pathway represented genes involved in iron uptake. It was decided that the focus of the rest of this study would be on this pathway. Iron uptake from the bloodstream is essential for virulence of *C. albicans* (Noble, 2013).

A pathway for iron uptake can be seen in Figure 5. The genes highlighted in this pathway are *RBT5*, *PGA10*, and *PGA7*. The mutants, *rbt5* and *pga10*, were identified from the second screen. The rest of these mutants, however, were not pulled from this screen due to the small coverage of this knockout library. Looking at the other mutants identified from the second screen, many were regulated by Hap43, which is a transcription factor that is induced in low-iron conditions (Hsu et al., 2011) and regulates the process of iron uptake (Noble, 2013). For future tests on this pathway the mutants were obtained from another lab and are isogenic strains.

RBT5 and *PGA10* are two redundant genes that code for extracellular structures responsible for acquiring hemoglobin and heme from the environment (Weissman and Kornitzer, 2004). *Pga7* acts intracellularly to shuttle the iron from the hemoglobin across the cell membrane into the cytoplasm, where the iron can be extracted. In order to understand how this pathway contributes to adhesion and possible interactions with Filastatin, several tests, including Atomic Force Microscopy (AFM) (Rosch, 2015) and interaction assays, were performed.

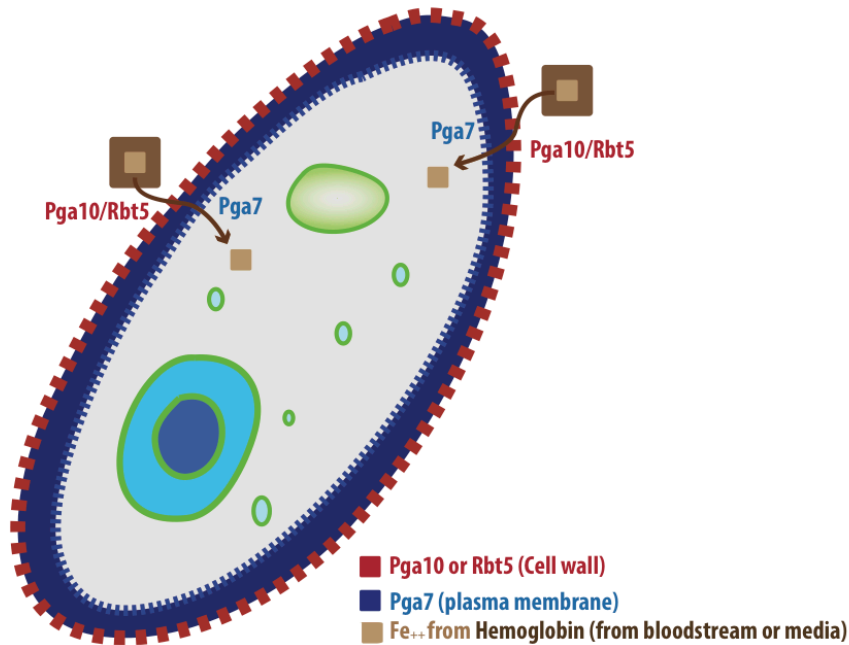


Figure 5: Iron-Uptake Pathway Working within the Cell. Rbt5 and Pga10 are extracellular structures, Pga7 works within the cell, and Hap43 is a transcription factor that regulates the process. Figure produced by R. P. Rao (Rao, 2015b).

Atomic Force Microscopy (AFM) Results

In order to understand how this iron pathway relates to adhesion, Atomic Force Microscopy (AFM) was used. The methods were developed by a group of MQP students, and thus not included here (Rosch, 2015). Briefly, the AFM measures the force that the cell applies to a glass surface. Each cell was tested on the glass 40 times and the trials were run in triplicate. The results (Figure 6) show that the iron mutants, *rbt5* and *pga10*, which are external structures, show reduced adhesion forces. The mutant *pga7*, which acts internally, shows a wild type level of adhesion. The mutant, *hap43*, normally acting as a transcription factor in the pathway, shows intermediate adhesion force between low levels and wild type adhesion forces.

These results show that there is a clear connection between the iron-uptake pathway mutants and adhesion, especially of the extracellular structures. Based on this information, it is important to know whether Filastatin affects the adhesion forces of the wild type strain. For this

reason, the adhesion force of wild type tested on glass and glass treated with Filastatin were measured. The results are shown in Figure 7.

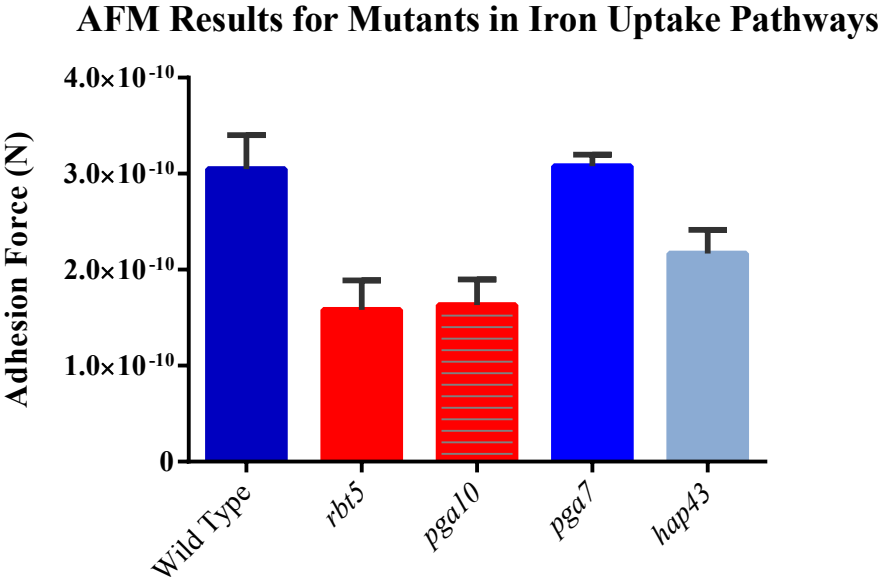


Figure 6: AFM Results for Mutants in the Iron-Uptake Pathway. Each mutant was run in triplicate. The error bars represent standard deviation (SD).

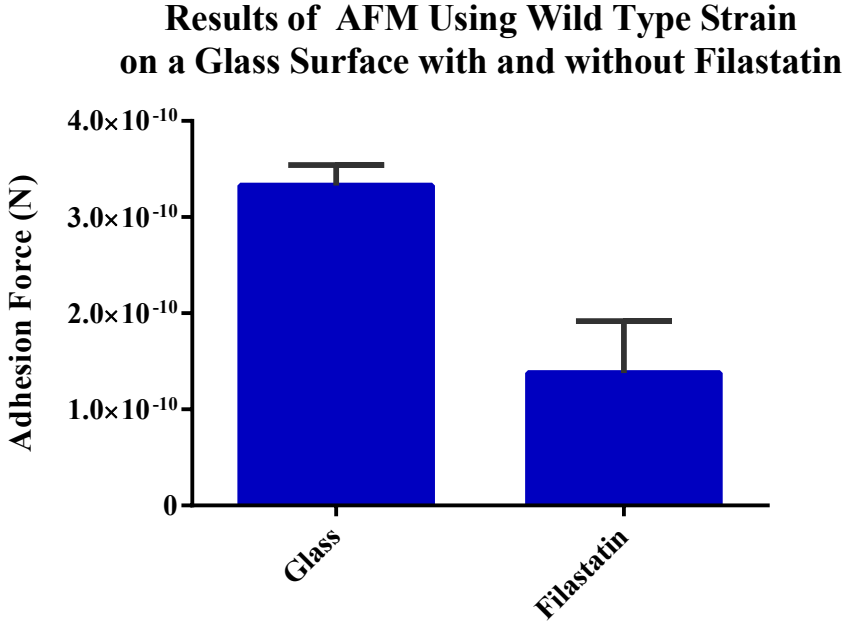


Figure 7: Adhesion Force Measurements using AFM of Wild Type Strain on Glass and Glass Treated with Filastatin. The error bars reflect SD.

A student's t-test was performed on the data, and the results show statistical significance between the two conditions ($p = 0.037$) (Rosch, 2015). This indicates that Filastatin is able to reduce the adhesion force of the *Candida*. Based on the data from the AFM, there may be a connection between iron-uptake pathways and adhesion. To understand this interaction, especially how Filastatin could be working within this pathway, interaction assays modeling adhesion in the presence of Filastatin and hemoglobin were performed.

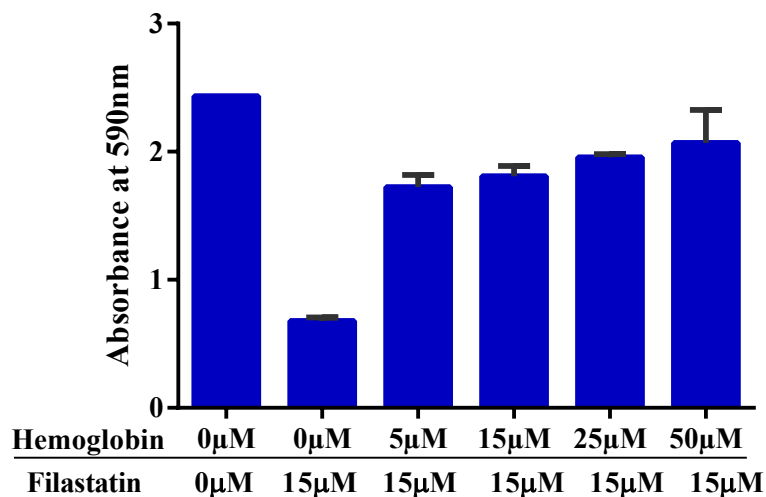
Interaction Assays: Hemoglobin and Filastatin

In order to test the theory that Filastatin may be interacting with the iron-uptake pathway, the interaction assay was performed varying the concentration of hemoglobin in the presence of constant concentration of Filastatin, as well as the inverse. The results, in Figure 8, suggest that there was an interaction between this pathway and Filastatin.

In Figure 8a, the concentration of Filastatin was held constant at 15 μM , and the level of hemoglobin was increased. When only Filastatin was in the system, the level of adhesion decreased from a baseline adhesion (no hemoglobin and no Filastatin). As the concentration of hemoglobin was increased, levels of adhesion increased. Figure 8b shows that when only hemoglobin was added to the system, the level of adhesion increased (compared to baseline), then adding Filastatin to the system decreased the adhesion. Figure 1 in Appendix C shows another view of the interaction assay when the same concentration of Filastatin and hemoglobin are added—the results are not simply additive, as one would suspect. This does, however, suggest that there is an interaction between the two.

Before confirming the interaction between hemoglobin and Filastatin, adhesion assays were performed to find the individual effect of both hemoglobin and Filastatin on *Candida*'s ability to adhere to plastics. Figures 9 shows increasing concentrations of Filastatin and hemoglobin, respectively. Increasing the concentration of Filastatin shows a steady decrease in adhesion, while increasing the concentration of hemoglobin shows a steady increase in adhesion. Both curves show a plateau at the same concentration, 10 μM , indicating that if this is a surface phenomenon, then *Candida*'s receptors may have been saturated. Otherwise, the maximal effect of altered adhesion occurs at the same concentration, 10 μM , which may indicate that the two compounds are vying for a similar receptor.

a. **Interaction Assay with Varying Concentrations of Hemoglobin**



b. **Interaction Assay with Varying Concentrations of Filastatin**

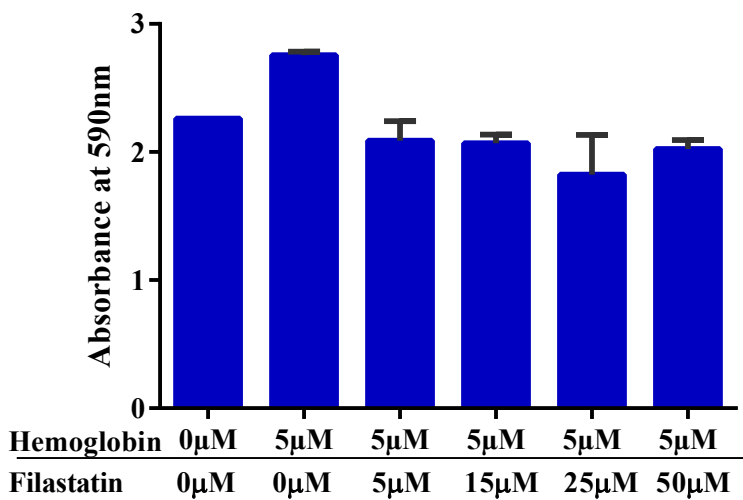


Figure 8: Interaction Assay Results for the Wild Type Strain. In both Panel a and b, the first well has no hemoglobin or Filastatin added, thus it is baseline adhesion. Panel a) shows a constant concentration of Filastatin (15 μM) in the last four wells, with increasing concentration of hemoglobin (0–50 μM). Panel b) shows a constant concentration of hemoglobin (5 μM) with increasing concentrations of Filastatin (0–50 μM).

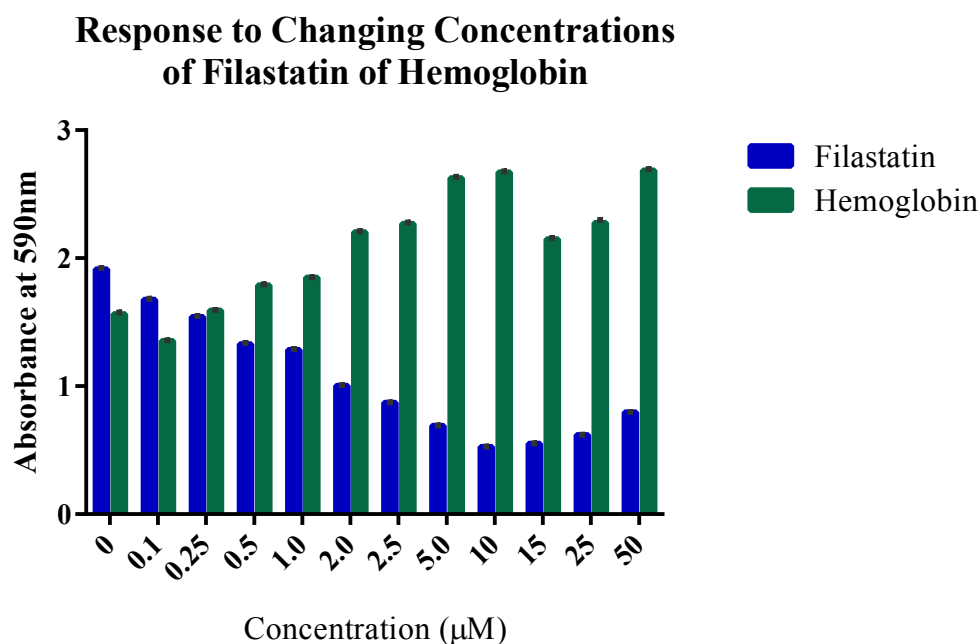


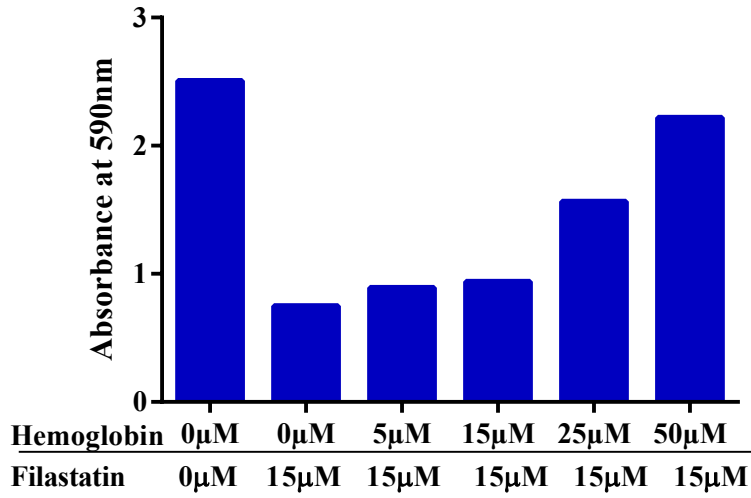
Figure 9: Wild Type Strain in the Presence of Increasing Concentration of Filastatin (0–50µM) and Hemoglobin (0–50µM)

These results suggest that Filastatin may be acting within the iron-uptake pathway to affect adhesion. In order to mimic the low iron conditions of the bloodstream, the effects of two iron chelators, bathophenanthrolinedisulfonic acid (BPS) and Ferrozine, were tested in the interaction assay (Figure 10). Both chelators produce a color change when bound to iron. BPS chelates extracellular iron, Fe^{3+} , while Ferrozine is known to chelate Fe^{2+} , which occurs intracellularly. The Ferrozine is capable of binding to the iron in hemoglobin. BPS shows no real effect on the interaction assay, as the increasing concentration of hemoglobin produces an increasing effect (Figure 10a). However, the Ferrozine is able to bring the adhesion level to baseline when in the presence of hemoglobin.

Figure 11 shows a biofilm assay prepared in glass tubes using several types of media. The results show that Ferrozine might be having an additive effect with the hemoglobin to increase adhesion of *Candida* to the plastic. This additive effect has also been shown for the transcriptional regulation of CaHMX1 (Pendrak et al., 2004). Additionally, it is possible that by chelating the iron (II), the Filastatin has less of an effect.

a.

Effect of An Iron Chelator, BPS, on the Interaction Assay



b.

Effect of An Iron Chelator, Ferrozine, on the Interaction Assay

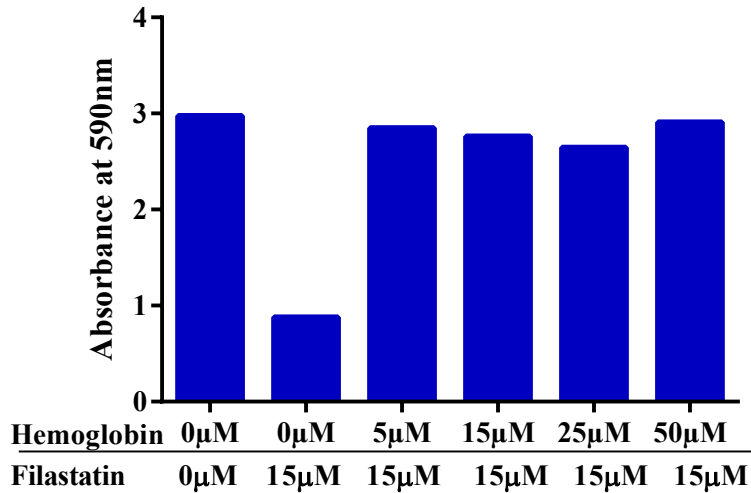


Figure 10: Effects of the two Iron Chelators on the Interaction Assay: Varying Concentrations of Hemoglobin. Both (a) BPS (1 mM) and (b) Ferrozine (1 mM) were used in the SC media for this assay to mimic low iron conditions of the blood. The rest of the assay was performed as stated before.

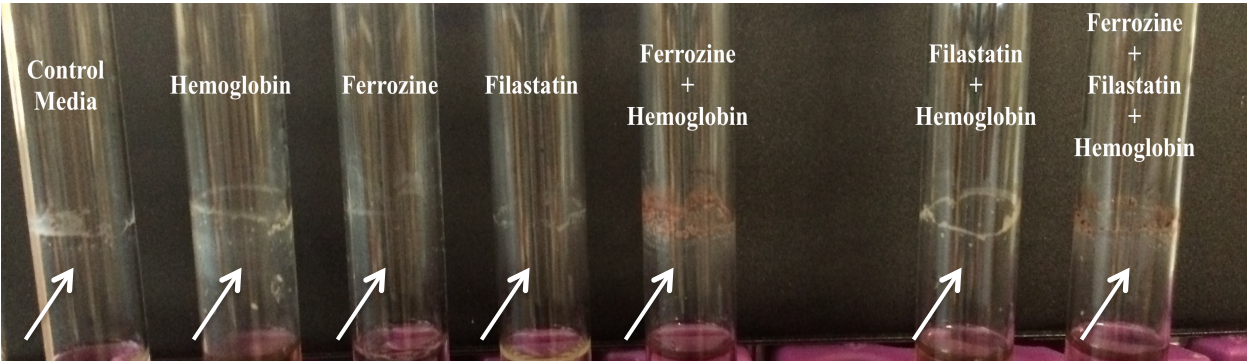


Figure 11: Biofilm Formation of a Wild Type Strain in Different Media Types. Cultures were grown at 30°C for 24 hours. Media types are listed above the biofilm growth, marked with an arrow. Hemoglobin was added exogenously at 10 µM concentration, Ferrozine at 1 mM, and Filastatin at 10 µM. Cultures were inoculated with 0.001 OD/mL of the wild type strain.

Candida albicans can form biofilms on glass tubes when suspended in normal, SC media. Hemoglobin induces biofilm growth even in the presence of Filastatin, which is known to prevent adhesion (an early step of biofilm formation). This result can be quantified using the biofilm assay, when the strains are grown in 96-well plates for 20 to 25 hours. This result is shown in Figure 12.

Based on Figures 11 and 12, the low-iron conditions coupled with available hemoglobin may induce biofilm formation, beginning by inducing adhesion (Figure 10b). The biofilm formation of the Ferrozine alone is not statistically different from the control media, indicating that the low-iron conditions without available hemoglobin or heme are not capable of inducing adhesion.

Although not cogent to this thesis, it was readily observable that only those biofilms formed with Ferrozine and hemoglobin, together, turned red in color, a function of Ferrozine bound to Fe^{2+} . Additionally, the cells, which would normally be free in solution, exhibited clumping. This could be due to the cells cohering within the media.

Filastatin is not able to prevent adhesion, shown in Figure 11, when hemoglobin and Ferrozine are also present. This indicates that Filastatin may not be as effective in a low-iron environment, like the bloodstream.

Biofilm Assay of Wild Type Strain in Different Media Types

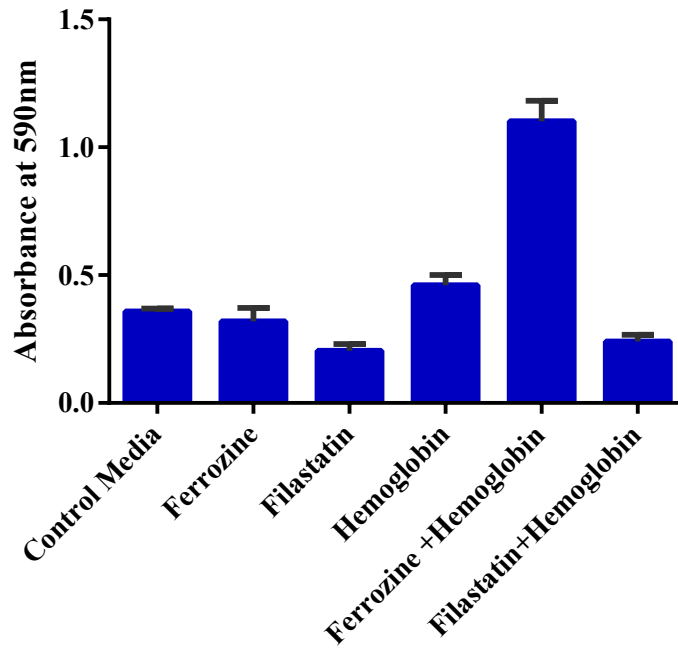


Figure 12: Biofilm Formation of Wild Type Strain in Different Media Types. Ferrozine is at a 1 mM concentration, while Filastatin and hemoglobin are at 10 μ M. The wells were inoculated with 0.01 OD/mL.

Discussion

Filastatin was discovered in 2013 in an effort to find additional drugs to fight *Candida albicans* infections, especially those caused by adhesion to the plastics of medical devices (Fazly et al., 2013). Before it can be used in the clinical setting, the target of the drug must be identified in order to better describe its mechanism of action. A reverse genetic approach was used and two screens were performed. Since there is no total knockout library for *C. albicans*, a mutant library enriched for transcription factors was used (Noble et al., 2010).

The original screen (Figure 3) aimed to find mutants when in the presence of the drug would show an exaggerated response, i.e., significantly more or less adhesion. From this screen, 233 mutants were isolated (Table 1). Of these mutants, several were involved in filamentation pathways, nutrient uptake, cellular responses, and many more pathways (based on GO analysis). Because this screen yielded such a large number of results, specific pathways were difficult to identify. A second screen, shown in Figure 4, was performed using the known function of Filastatin as a tool for the discovery of the target. This screen yielded only 43 genes (Table 2). The pathways isolated from this screen were adhesion and biofilm formation, which validated our screen, but, also, iron uptake. Because it was already known that Filastatin prevents adhesion, the iron-uptake pathway became the focus for the remainder of the project.

The first step of the project was to confirm that the iron-uptake pathway is connected to adhesion processes. Therefore, the mutants of an iron-uptake pathway, *rbt5*, *pga10*, *pga7*, and *hap43* were tested using the AFM, which measures the force that the cells exert on the surface (Figure 6). The results showed that mutants, *rbt5* and *pga10*, which are missing extracellular structures responsible for acquiring hemoglobin/heme from the environment, are responsible for some adhesive force. It is known, in the field, that mutants lacking Rbt5, Pga10, or other similar proteins form weaker biofilms with less extracellular matrix (Kronstad et al., 2013). This result, in conjunction with the literature, indicates that the process of binding hemoglobin/heme may mediate adhesion. Additionally, according to Figure 7, Filastatin acts to reduce the adhesive force of the *Candida* on the glass surface. This suggests that Filastatin may be acting on the surface of the cell.

Based on the results of the screen, it is possible that Filastatin is somehow interacting with the proteins of this iron-uptake pathway. More assays uncovering the relationship were performed using the CV stain in both an adhesion and biofilm assay. When hemoglobin was

added to the system, there was an increase in adhesion; the converse was true when Filastatin was added in increasing concentrations (Figure 9). If Filastatin is acting on the surface of the *Candida*, then both hemoglobin and Filastatin may be vying for the same receptor. Figure 8 and Appendix C show that there is an interaction between the two when both drugs are added to the system. If they were acting independently within their own mechanisms, then it would be expected that the effect of the two would be additive. That is, the adhesion promoting the effects of hemoglobin combined with the inhibitory effects of Filastatin would lead to an intermediary level of adhesion. In Figure 8a, when 15 μM of both hemoglobin and Filastatin are added, the adhesion is not restored to baseline. However, in Figure 8b, when 5 μM of each is added to the system, the result is baseline adhesion. This may indicate that there is an interaction or that hemoglobin is less effective at lower concentrations. Future experiments to test this interaction may include testing more concentrations of hemoglobin and Filastatin, based on Figure 9. Additionally, a test during which *Candida* is allowed to incubate with either hemoglobin or Filastatin followed by addition of the other may help elucidate whether or not these ligands are competing for the same receptor. This would help to answer two questions: 1) are they acting within the same receptor, and if so, then when one is able to fill the receptors, can the other still be effective? and 2) Will this show the same level of effectiveness?

The bloodstream is normally considered low-iron, thus two iron chelators, BPS and Ferrozine, were used to mimic this condition. BPS binds to Fe^{3+} , which is found extracellularly, and normally found within Ferritin. Figure 10a shows that BPS does not seem to effect the results of the interaction assay. On the other hand, Ferrozine, which sequesters Fe^{2+} (Sheftel et al., 2012), is able to increase adhesion to baseline when in the presence of hemoglobin. An additive effect between Ferrozine and hemoglobin has been seen in terms of the gene *CaHMX1* as well. *CaHMX1* is a heme oxygenase, which is necessary for *C. albicans* to survive when heme is the only available source of iron (Pendrak et al., 2004). Iron-uptake related genes have also been shown to affect filamentation (Xu et al., 2014), which is a precursor to biofilm formation.

Biofilm formation was modeled in glass tubes incubated at 30°C (Figure 11). Ferrozine media showed no difference compared to the control media. This indicates that although the iron is being chelated away from the media, adhesion is still occurring, at least at control levels. When hemoglobin is added to the system in a concentration of 10 μM , the adhesion (and

therefore biofilm formation) increases significantly (Figures 10b and 12). *In vivo*, the bloodstream is a low-iron environment, which can be modeled *in vitro* using Ferrozine in the adhesion assay and biofilm assay. The Filastatin was able to limit biofilm formation in the presence of hemoglobin, but in the low-iron conditions, biofilm was still able to form (Figure 11). This is an indicator of how it may perform clinically, although this result will need to be quantified in the Biofilm Assay (plastic). However, the AFM studies (Figure 7) show that Filastatin is capable of limiting the adhesive force of *Candida* to glass surfaces. This may indicate that Filastatin's purpose should be to coat the medical devices only, rather than acting within the bloodstream as a drug. Future studies should include testing the effectiveness of Filastatin to reduce the adhesive forces on plastics that medical devices are commonly made of. Additionally, *in vivo* testing, using murine catheter model (Andes et al., 2004) will be important to understand how Filastatin will act within a realistic model of infection both as a surface coating on the catheter and as an injectable drug.

Other future studies might include biochemical or binding assays, which might require collaboration with a biochemist to prove that Filastatin requires Fe^{2+} . Additionally, one could flood free iron to the system with Filastatin, either in the form of Ferritin, Fe^{3+} , or a ferrous source of iron. This would show that when Filastatin is in the presence of Fe^{2+} (and not Fe^{3+}), the cells are not able to adhere as well. In other words, available Fe^{2+} would enhance the effect of Filastatin.

A significant amount of testing will need to occur before Filastatin can be implemented into a clinical setting. However, this study has shown that Filastatin may be acting within the iron-uptake pathway, which is important for both virulence and adhesion. Additionally, Filastatin is not able to prevent biofilm formation in low-iron conditions, which mimic the bloodstream. A summary of these results can be found in Appendix D.

Chapter 3: Phenomics Panel on Several Clinical Isolates of *Candida albicans*

Introduction

Many systems can be used to study *Candida albicans* including: *in vivo*, *ex vivo*, and *in vitro* systems. An extensive phenomics report of clinical isolates is not often done. For this investigation, several phenotypes of two clinical isolate series, taken in a time course, were studied. The list of strains, including the clinical isolates and their sources, are shown in Table 3.

As a follow-up to the Filastatin experiments, the ability of the clinical isolates to adhere to plastic was tested. *Candida albicans* is able to adhere and form biofilms on both abiotic and biotic surfaces (Hogan et al., 2004; Mayer et al., 2013). Plastics, such as those used to manufacture medical devices, are common substrates for biofilm formation. Mature biofilms are more resistant to drugs and host responses (Li et al., 2012). The ability to adhere to abiotic surfaces would confer an advantage, thus more virulent strains would be better able to adhere to plastic.

The clinical isolates were tested for virulence using *C. elegans*, a high-throughput model organism that has been used to monitor infection through several phenotypes (Ewbank, 2002; Garsin et al., 2003; Hodgkin, 2000; Pukkila-Worley et al., 2011). In this study, a visible phenotype, known as deformed anal region (Dar), was monitored. Dar is an inflammation of the post-anal region, which begins to appear by Day 3 (Jain et al., 2009). Additionally, the lifespan of *C. elegans* infected with each of the clinical isolates was tracked in a survival assay. It was hypothesized that any clinical isolate present during active infection would exhibit enhanced virulence.

In addition to *in vivo* assays used to measure virulence, an *ex vivo* assay using the cultured murine macrophages, RAW264.7, was performed. Macrophages are one of the host's first defense mechanisms, and they are able to engulf the fungi. The nutritional environment that the fungi face when engulfed is different and harsh (Filler and Sheppard, 2006; Lewis et al., 2012; Mayer et al., 2013), and thus, virulent *Candida* must be able to survive several conditions. The ability of the clinical isolates to survive when co-cultured with the macrophages can be

measured. More virulent strains are able to survive better and may even be capable of filamenting within the macrophages, causing them to burst (Lewis et al., 2013).

Yeast cells are capable of performing a dimorphic transition between planktonic yeast cells and hyphal forms. Both forms are vital for pathogenicity (Mayer et al., 2013). It has been shown that the hyphal are more capable of invading both *in vitro* agar and epithelial cells *in vivo*. Finally, a host of *in vitro* phenotypes were tested. Morphology on starving media and the cell's ability to invade agar were monitored.

Because *Candida* are able to disseminate throughout the body to many organs, where the nutritional availability changes, several stressors were tested *in vitro*. These included metals, drugs, as well as varying temperatures. Metals, like iron, zinc, and copper, are known to be essential for growth of *C. albicans*, but the mechanisms by which the fungi acquire them are still poorly understood. In addition to metals, the growth in the presence of several drugs was monitored. Fluconazole is the most popular treatment for *C. albicans*; however, resistance is becoming a serious problem (Control, 2013). The final set of *in vitro* phenotypes was of varying temperatures, as heat shock proteins protect the yeast from death when the environmental temperatures change.

Looking at the phenotypes present from each of the clinical isolate series, intraspecific comparisons can be made within each series. Additionally, the information regarding the host allows for interspecific comparisons.

Table 3: Sources of Strains including Clinical Isolates. Patient names (V and B) were assigned for ease of understanding.

Sample	Ploidy	Source	Patient	
SC5314	Diploid	Wild type strain, laboratory derived reference strain	N/A	
PN1	Tetraploid	Vaginal swab sample	Patient V*	
PN2	Diploid	Commensal cheek swab		
FH1	Diploid	Fecal samples	Patient B**	
FH2	Diploid			
FH3	Diploid			
FH5	Diploid	Blood samples		
FH6	Tetraploid			
FH8	Diploid			
RBY18	Tetraploid	Laboratory strain tetraploid		N/A
RBY16	Diploid	Parent diploid of laboratory strain RBY18		N/A
MMY304	Diploid	Parent diploid of laboratory strain RBY18	N/A	

*Patient V had chronic vaginitis and was treated with antifungals.

**Patient B received a bone marrow transplant and was also treated with antifungals.

Materials and Methods

Growth Conditions for Yeast and Worms

Yeast strains were maintained on YPD plates. Fresh plates were struck weekly from glycerol stocks, which were kept at -80°C . The plates were stored at room temperature and wrapped in paraffin (Sherman, 1991). Before each assay, the strains were grown in liquid media overnight, spinning at 30°C .

The wild type strain of *C. elegans*, N2, were maintained at 20°C on normal growth media (NGM) agar plates (Stiernagle, 2006). The plates were seeded with OP50 and the worms regularly transferred to fresh plates to avoid starving.

Egg Preparation

Worms were grown for four to five days on NGM agar with *E. coli* (OP50) at 20°C . Eggs were washed off the plate with M9 buffer and centrifuged at 900 g for two minutes. The pellet was resuspended in a 1:4 dilution of commercial bleach (5.25%) containing 0.25 M sodium hydroxide solution, mixed gently by inversion, and centrifuged for two minutes at 2000 g. The pellet was washed with M9 and centrifuged at 2000 g. The egg suspension was diluted with M9 and enough mix to obtain approximately 20 worms per plate were plated.

Dar Assay

E. coli and yeast strains were grown overnight at 37°C and 30°C , respectively. Culture aliquots were centrifuged at full speed for 10 minutes, washed with sterile water, and resuspended to a final concentration of 200 mg/mL and 10 mg/mL, respectively. A mixture of 10 μL of a 50 mg/mL streptomycin sulfate stock, 7 μL of an amino acid solution (containing R-H-L-M-W, adenine, and uridine), 2.5 μL of the *E. coli* mix, and 0.5 μL of the yeast mix was prepared. Worms were prepared according to “Egg Preparation.” Plates were stored at 20°C and observed beginning on day 3 until day 5, recording the number of worms displaying the phenotype (Jain et al., 2009). A z-test was used to check the statistical significance between the members of the PN series and among the members of the FH series.

Survival Assay

For survival analysis, test plates and *C. elegans* eggs were prepared according to the “Egg Preparation” and “Dar Assay” methods. Each plate was seeded with 20–25 eggs. Beginning on the third day after plating the eggs, the number of dead and live worms was recorded on each plate each day. Live worms were transferred to a new plate as necessary to avoid confusing the worms with their progeny. Subsequent plates were of the same composition as the original test plates. Graphpad prism was used to create and analyze the Kaplan Meier survival curves. Significance, as defined by a p-value less than 0.05 was assessed using the Gehan-Breslow test. Worms that left the plate were “censored,” i.e., removed from the counts on subsequent days. The Gehan-Breslow test assumes that the data from early survival times are more accurate than data from later times and weights them accordingly.

Macrophage Assay

RAW 264.7 (ATCC) was used for this assay. The cell line was maintained in Dulbecco’s Modified Eagle Medium (DMEM) supplemented with 10 percent fetal bovine serum (FBS) and one percent penicillin/streptomycin. Macrophages, upon reaching 80–90 percent confluence, were scraped and brought up in supplemented DMEM. 2×10^6 cells were plated in three wells of a six-well plate and allowed to adhere for five hours. *Candida* strains were grown in YPD media overnight at 30°C and diluted 1:10 with fresh media, then allowed to grow for another five hours. *Candida* cells were counted, suspended in DMEM, and added to the plate containing macrophages in a ratio of 1:15 macrophage to a final volume of 2 mL. The yeast strains were grown in parallel in the other three wells of the six-well plate without macrophages to calculate percent survival. Plates were incubated overnight at 37°C and five percent CO₂. Cells were brought up to 24 mL in a 50 mL conical tube using 0.05% Triton X-100 (v/v) in water to osmotically lyse the macrophage cells. Conical tubes were vortexed for one minute and serial dilutions were carried out immediately after. Two dilutions were plated on YPD plates and grown overnight at 30°C. Colony forming units (CFU) were counted and percent survival was calculated by taking the ratio of CFU from the co-culture of *Candida* and macrophage to the CFU obtained for *Candida* alone.

***In vitro* Phenotypic Profiling Assays**

Plates were prepared using synthetic complete (SC) media (Sherman, 1991) supplemented with 0.15% glucose, amino acids (R-H-L-M-W), adenine, and uridine. Drugs and stressors were added as necessary to the liquid media before pouring.

All of the clinical isolate strains were obtained from Dr. Judith Berman at the Tel Aviv University, Israel. Reference strain for the tetraploid and its diploid parents were obtained from Richard Bennett at Brown University. Two to three days before beginning each assay, strains were struck from frozen stock onto YPD plates and grown at 30°C overnight. These plates were stored at room temperature for one week. The night before the assay, a liquid culture in YPD media was started and incubated at 30°C. Strains were centrifuged and resuspended in water to 1 OD/mL and serial dilutions were made using dH₂O as well. Using a multichannel pipet, 5 µL of each dilution was added to the plates for each strain. A wild type reference strain was included with each set of clinical isolates. Plates were stored at 30°C unless otherwise stated. Plates were photographed with an iPhone camera one, three, and five days post spotting. The pictures were analyzed using ImageJ software. Heat maps were created for each condition using Excel.

Adhesion Assay

Single colonies were picked and inoculated into 5 mL cultures of SC + 0.15 percent glucose media and grown overnight in a rotating wheel. The optical density (OD) of the cultures was then measured at OD₆₀₀ nm. Cultures were spun down and resuspended in fresh SC + 0.15 percent glucose to a final concentration of 0.5 OD/mL. 200 µL of 0.5 OD/mL *C. albicans* strains were pipetted onto 96-well flat-bottom polystyrene plates. Plates were covered with aluminum foil and incubated at 37°C for four hours. After four hours of incubation, plates were decanted, and 40 µL of 0.5 percent crystal violet (CV) stain was added to each well. The plates were covered and left at room temperature to incubate for 45 minutes. Plates were then decanted and washed by submersion 10 times in an ice bucket filled with dH₂O, changing the water every five washes. Plates were tapped onto a paper towel to remove residual dH₂O, and 200 µL of 75 percent MeOH was added to each plate and incubated at room temperature for 30 minutes. The plates were then read at 590 nM to detect relative absorbance.

Results

Several phenotyping assays were performed in this study comprising *in vivo*, *ex vivo*, and *in vitro* tests of the clinical isolates. For each assay, the clinical isolates listed in Table 3, were run in parallel to the reference lab strain, SC5314. This strain began as a clinical isolate, but has been maintained in many laboratories since the late 1960s (McRipley et al., 1979), and thus has most likely lost the characteristics of clinical isolates. However, because it is commonly used as the wild type strain in most experiments involving *C. albicans*, for this study it will be a reference strain. Additionally, SC5314 acted as an experimental control for the *in vivo* and *ex vivo* assays to make sure that they were working properly as this strain has been tested previously. The resulting information of these assays for both sets of clinical isolates were then analyzed to make important connections about their virulence.

***In vitro*: Adhesion Assay**

Initially, the clinical isolates were tested for the ability to adhere to plastics (Figure 13). It is possible that cells with increased capacity for adhesion would be more likely to invade the bloodstream (Bliss et al., 2012). Additionally, adhesion is the first step in biofilm formation, which can be modeled by this assay (Figure 2). This is important because *C. albicans* is capable of forming biofilms on plastic medical devices. According to Figure 13, PN1 shows significantly more adhesion than PN2 based on an unpaired t-test ($p < 0.0001$). Of the FH Series, FH3 shows significantly more adhesion, which indicates that it is more virulent than the other strains in this series, analyzed by a one way ANOVA, with Tukey's multiple comparison test.

***In vivo*: Dar Assay**

C. elegans is a useful model for studying virulence of fungal pathogens, such as *C. albicans*. The deformed anal region (Dar) phenotype (Jain, 2013) presents three days post-infection, and can be seen until death. However, useful comparisons stop after day five when the plates become overcrowded with progeny and the worms begin to die off. Beginning on day four, SC5314, the reference strain, shows close to 100 percent Dar. Any amount less than this on day four would indicate a less virulent strain. In addition, 100 percent Dar on day three would

indicate increased virulence compared to the reference strain. Figure 14 shows the results of testing the clinical isolates for Dar on day four and five.

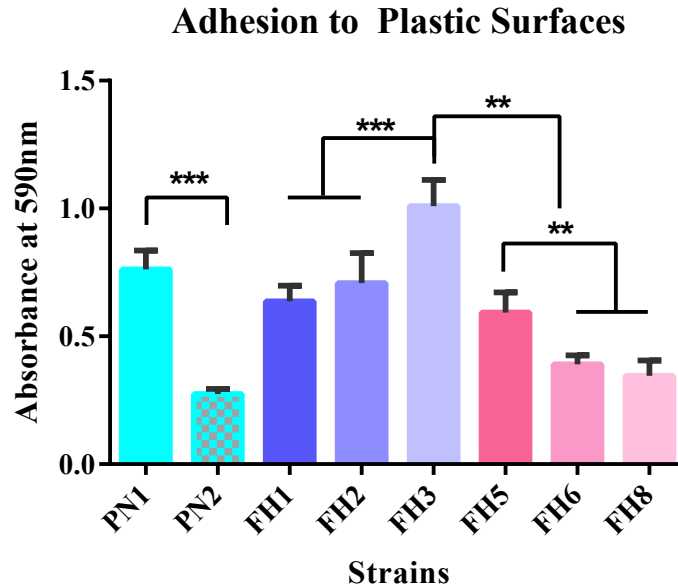
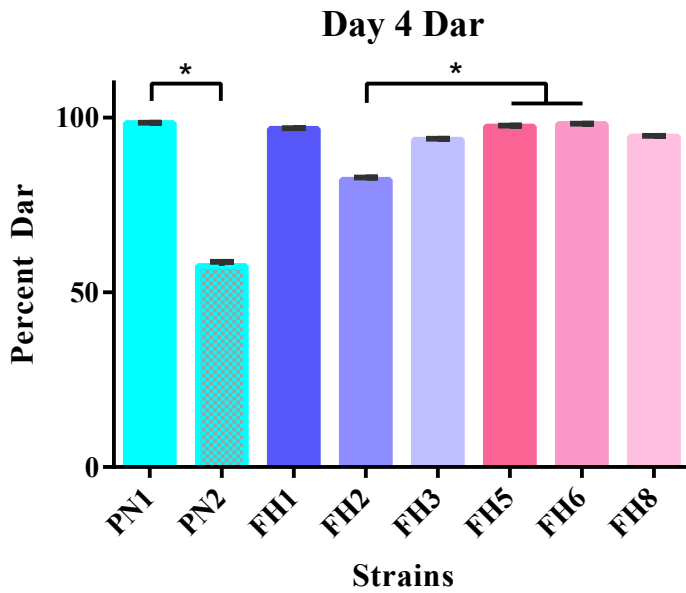


Figure 13: Adhesion, Measured by Absorbance at 590 nm, of Each of the Clinical Isolate Strains. Error bars are a measure of SEM.

In Figure 14a PN2, the commensal strain, shows significantly less ($p < 0.05$) Dar phenotype as compared to its counterpart PN1, which was isolated during an active infection episode. This indicates that PN2 is less virulent. The phenomenon persists through day five (Figure 14b) when PN1 becomes 100 percent.

The FH series was also tested in the Dar assay. These strains have similar virulence as shown in Figure 14a, day four. FH2 is the only strain below 90 percent, making it significantly different from FH5 and FH6 ($p < 0.05$). However, on day five, all strains reach 100 percent. FH2 may be less virulent than some of the other strains, although the results are far less clear than those of the PN series. It was necessary to perform the second *in vivo* assay modeling lifespan in the presence of the drug.

a.



b.

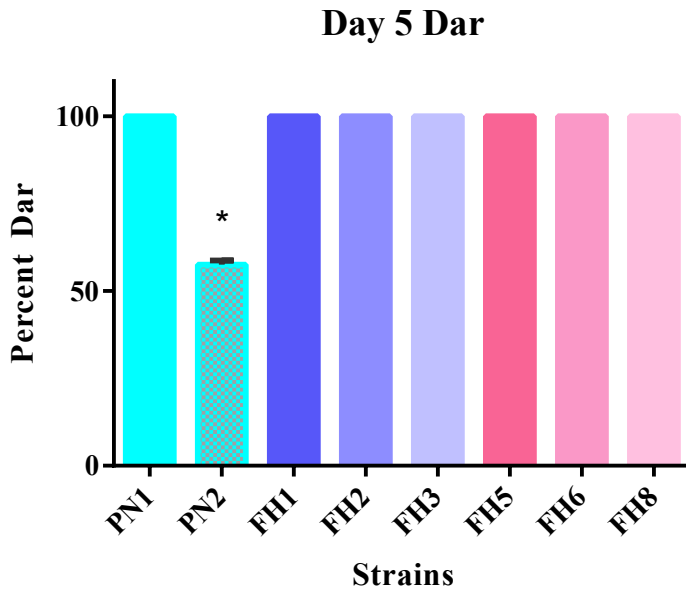


Figure 14: a) Day 4 Dar Measurements of the Reference Strain, SC5314, the PN Series, and the FH Series. b) Day 5 Dar measurements of the reference strain, SC5314, the PN Series, and the FH Series. Error bars represent standard error of proportion in these figures.

In vivo: Survival Assay

In addition to the Dar assay, virulence can be measured using the survival assay, which models the nematode's lifespan by substituting their normal food with yeast. Uninfected, wild type *C.*

elegans, N2, live for 21 days at 20°C. The clinical isolates survived for only 14–16 days, with the exception of PN2, which maintained 50 percent survival by day 16. Two types of statistical analysis were used: the log rank test and the Gehan-Breslow test. The log rank test is most commonly used in the field and assumes that the ratio of hazards is the same at each time point, while the Gehan-Breslow test places a greater value on the deaths in the early days. Only the p-values of the Gehan-Breslow test are reported within the text, but Table 1 in Appendix E shows a compilation of the p-values from both tests.

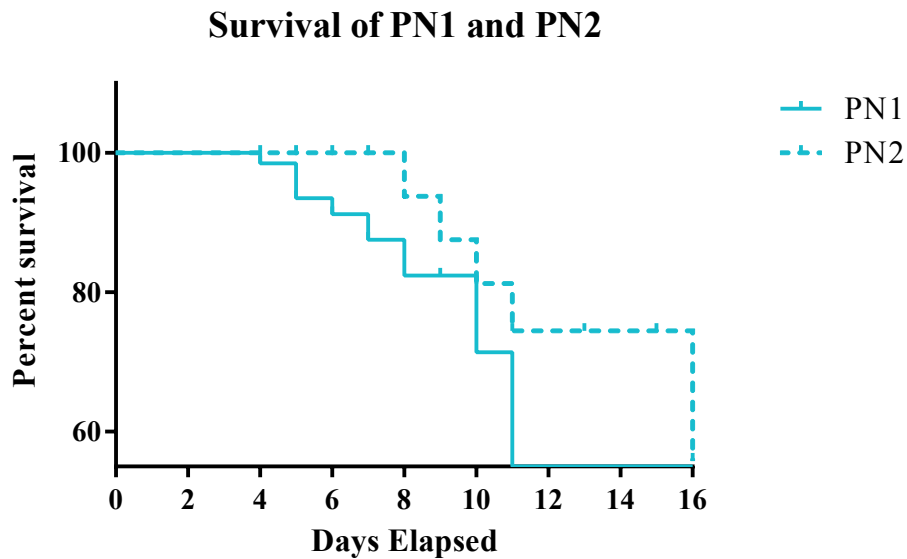


Figure 15: Survival Comparison between PN1 and PN2

According to Figure 15, by day 11, 50 percent of the worms exposed to PN1 had died, which can be compared to worms infected with PN2, where 50 percent of the infected worms had survived until day 16. These results indicate that PN2 is significantly less virulent ($p = 0.0049$) than its counterpart, mimicking the results from the Dar assay. Median survival times, shown in Table 4, are also a useful tool for indicating virulence. For instance, the median survival time for PN1 is 12.0 days, while the median survival time is undefined for PN2. The worms living in the presence of PN2 tended to live longer and thus had more time to crawl off the plate. By day 16, there were no longer any worms to score on the plate.

Strain	Median Survival Time
PN1	12
PN2	Undefined
FH1	9
FH2	9
FH3	10
FH5	10
FH6	9
FH8	9

Table 4: Median Survival Time for Clinical Isolate Strains in Survival Analysis

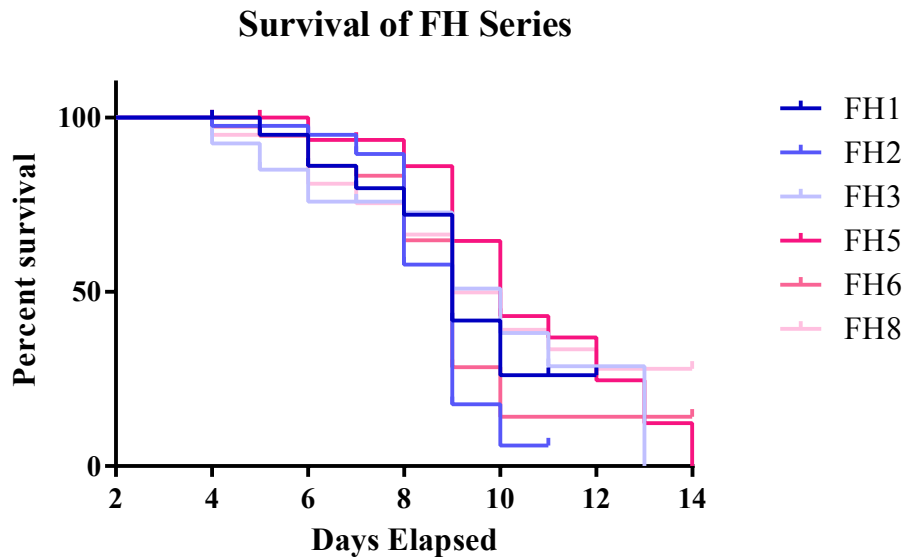


Figure 16: Survival Analysis of the FH Series

The FH series was also tested in survival, and visually, the results, shown in Figure 16, appear closely matched for each strain. According to the Gehan-Breslow test, the curves are significantly different ($p < 0.0001$). FH3 shows the most death early on, killing 25 percent by day four. FH5 takes eight days to reach this same percentage of death. However, the median survival times are not different. As shown in Table 4, the median survival is nine days for FH1,

FH2, FH6, and FH8, while FH3 and FH5 have a median survival time of 10 days. Based on the data from the Dar and survival assays, there is little difference in the virulence of the FH series.

Ex vivo: Macrophage Assay

To further characterize the pathogenicity of the clinical isolate series, an *ex vivo* assay was used to measure survival of *C. albicans* when exposed to cultured murine macrophages, RAW 264.7. This *ex vivo* test is an effort to mimic the biology of the host–pathogen interaction. It is known that the macrophages engulf the yeast cells and either kill or render them incapable of multiplying (Lewis et al., 2012). A strain that shows a high ratio of colony forming units (CFU) of co-culture with macrophage to CFU of *Candida* alone is more virulent as the macrophages have less of an effect on that strain. However, if the macrophages are capable of killing a high number of the yeast cells, then the ratio would be lower, and the strain less virulent.

Figure 17a shows that PN1, at 63 percent survival in the presence of the macrophage, is significantly more virulent than PN2, the commensal strain, which showed only six percent survival. Similarly to the survival assays, the clinical isolates in the FH series all show relatively similar survival in the presence of the macrophage, less than 10 percent (Figure 17b). However, of this group, FH3 is shown to be the most virulent, which can be correlated to the early days of the survival assay. Interestingly here, FH1 is less virulent, but in both the Dar and Survival assays, FH1 showed similar virulence levels to the other strains in the series.

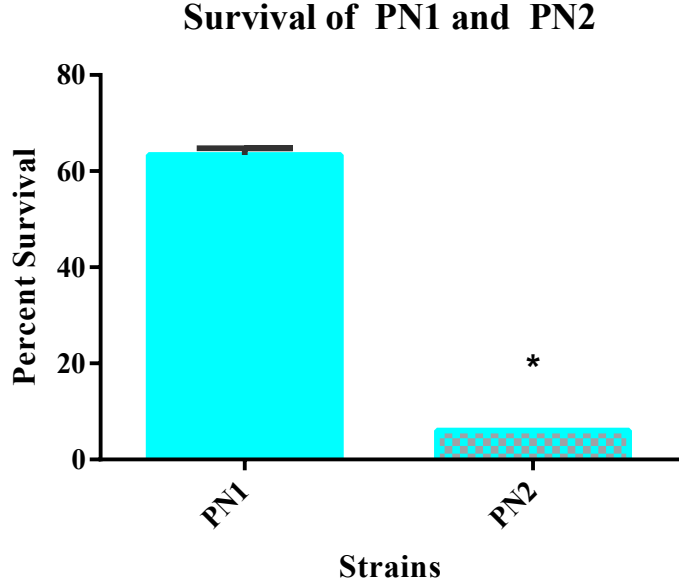
Based on the data from the *in vivo* and *ex vivo* assays, PN1 is clearly more virulent compared to PN2. This is likely because it was isolated from an active infection. The FH series all show similar levels of virulence in each of the previous assays. The *in vitro* tests can be used to elucidate some differences among the strains, which could provide useful information for treatment.

In vitro: Morphology

There are several ways to examine the morphology of yeast. The first is by plating the yeast on spider media (Lo et al., 1997) to induce filamentation, shown in Figures 18 and 20. The second is through an invasion assay, which can potentially model invasion of the *Candida* into the bloodstream through the blood vessels or the epithelial layers of the gut (Dieterich et al., 2002). To test invasion, cells were spotted on agar plates and incubated at 30°C. Then the cells were

scrubbed off the surface under a gentle stream of water. Attached cells were photographed (Figures 19 and 21).

a.



b.

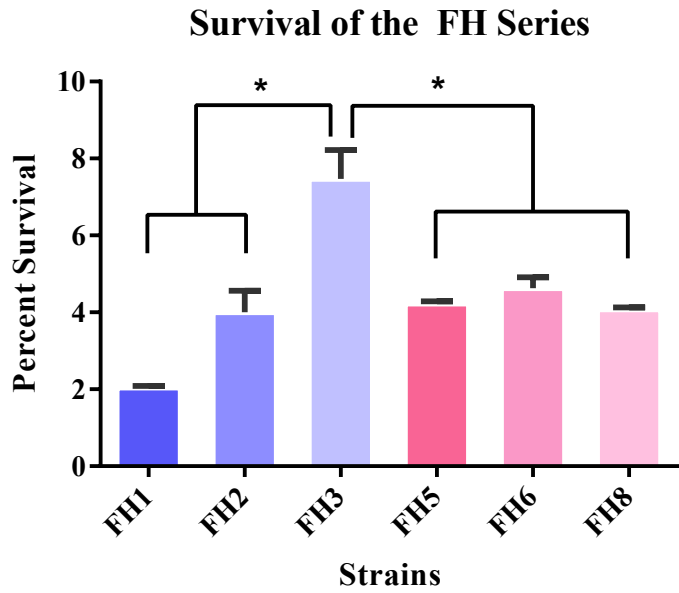


Figure 17: Results of the *Ex Vivo* Macrophage Assay for a) the PN series and b) the FH series. Percent survival is found by taking the ratio of co-cultured yeast with macrophages to yeast alone. Error bars represent SEM.

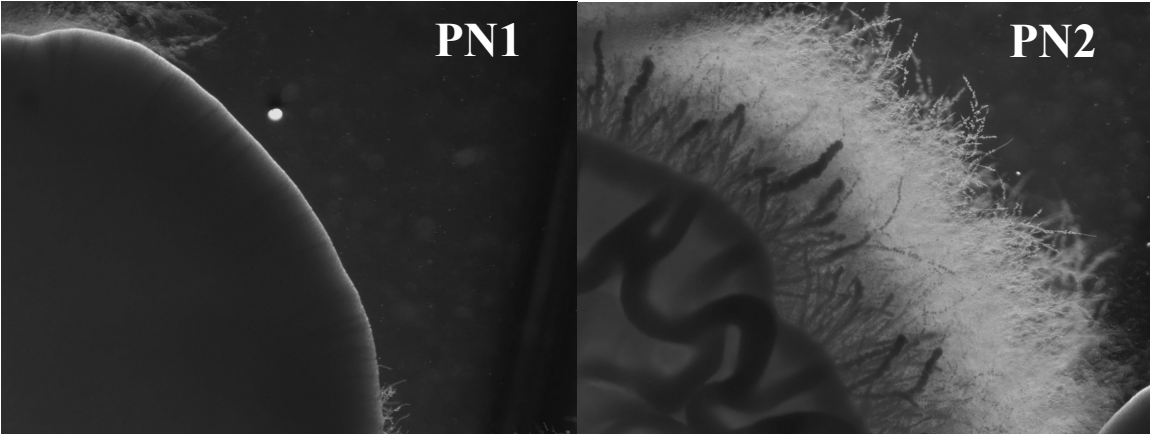


Figure 18: Attached Cells. Filamentation forms under starved conditions on spider media of PN strains grown at 30°C for 10 days.

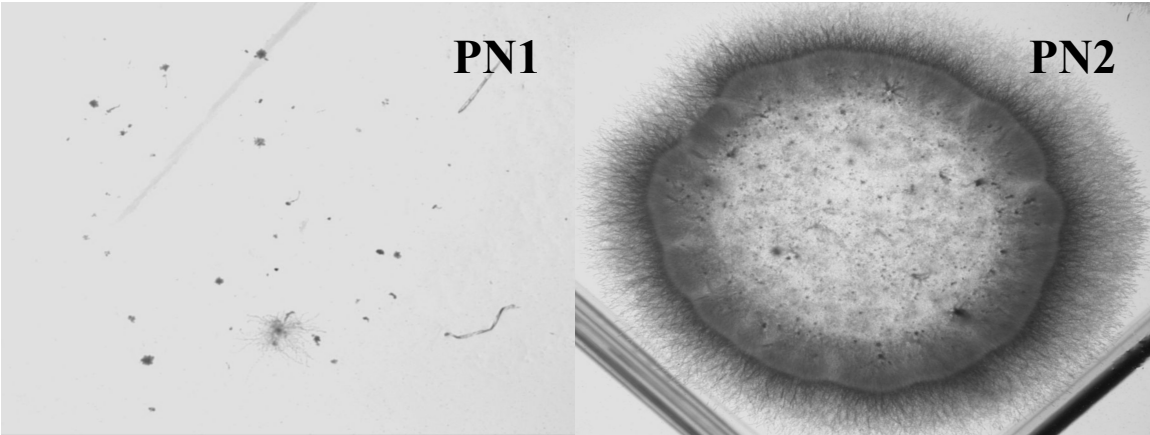


Figure 19: Invasion of PN1 and PN2. Samples were grown on YPD Plates for 10 days at 30°C and run under distilled water to clean off the spot, revealing the invasion into the soft agar.

According to Figure 18 and 19, PN2 is more filamentous and invasive than PN1. This may seem counterintuitive to results presented earlier using the *C. elegans* model and the *ex vivo* macrophage model of infection. PN1, which was isolated during an infection, was more virulent than PN2, the commensal strain. Filamentous cells are important for attachment, however normal yeast cells are important for dissemination of the infection (Ariyachet et al., 2013; Filler and Sheppard, 2006). It is thought that mucosal infections, like thrush or vaginitis, are more commonly associated with the yeast cell form, whereas internal organ infections require the filamentous form.

In the FH series, FH2, FH3, and FH6 showed limited ability to filament compared with FH1, FH5, and FH8. It is interesting to note that FH1, FH2, and FH3 were isolated from fecal samples, while FH5, FH6, and FH8 came from blood samples. This may correlate with the

results from the PN series, as the strains that are more likely infections of the lining of the intestine—FH1, FH2, and FH3—will likely present in yeast budding form (Figure 20). These strains also showed less invasion of the soft agar (Figure 21) than the strains that were isolated from the patient’s blood—FH5, FH6, and FH8.

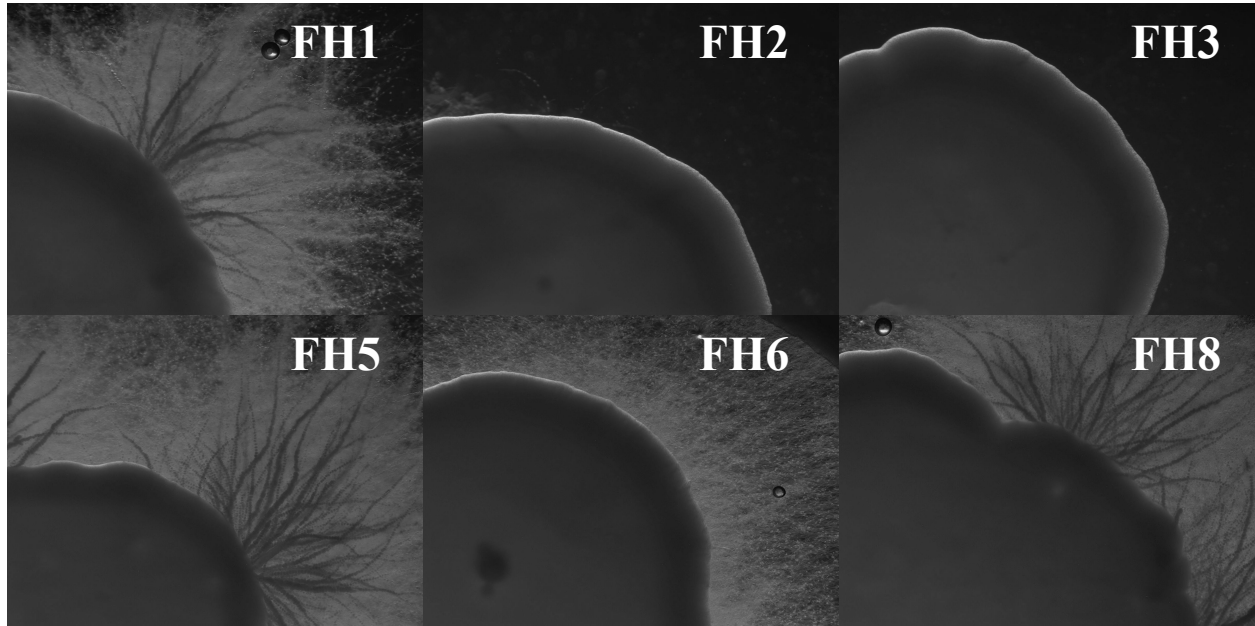


Figure 20: Attached Cells. Filamentation forms on spider media of the FH series and reference strains. The samples were grown at 30°C for 10 days.

***In vitro*: Stress Conditions**

Phenotypic profiling, using *in vitro* plate modeling, has been performed on several *Candida albicans* mutants in order to identify the function of many transcriptional regulators (Homann, 2009). In this work, a similar, phenotypic profiling was performed in order to elucidate the differences among strains acting within a single patient. It is possible that this work could be used as a model for profiling other clinical isolates to better inform treatment plans. Additionally, the heat maps produced show that the strains from a single patient do not reflect a uniform phenotype, indicating that each new infection must be treated differently.

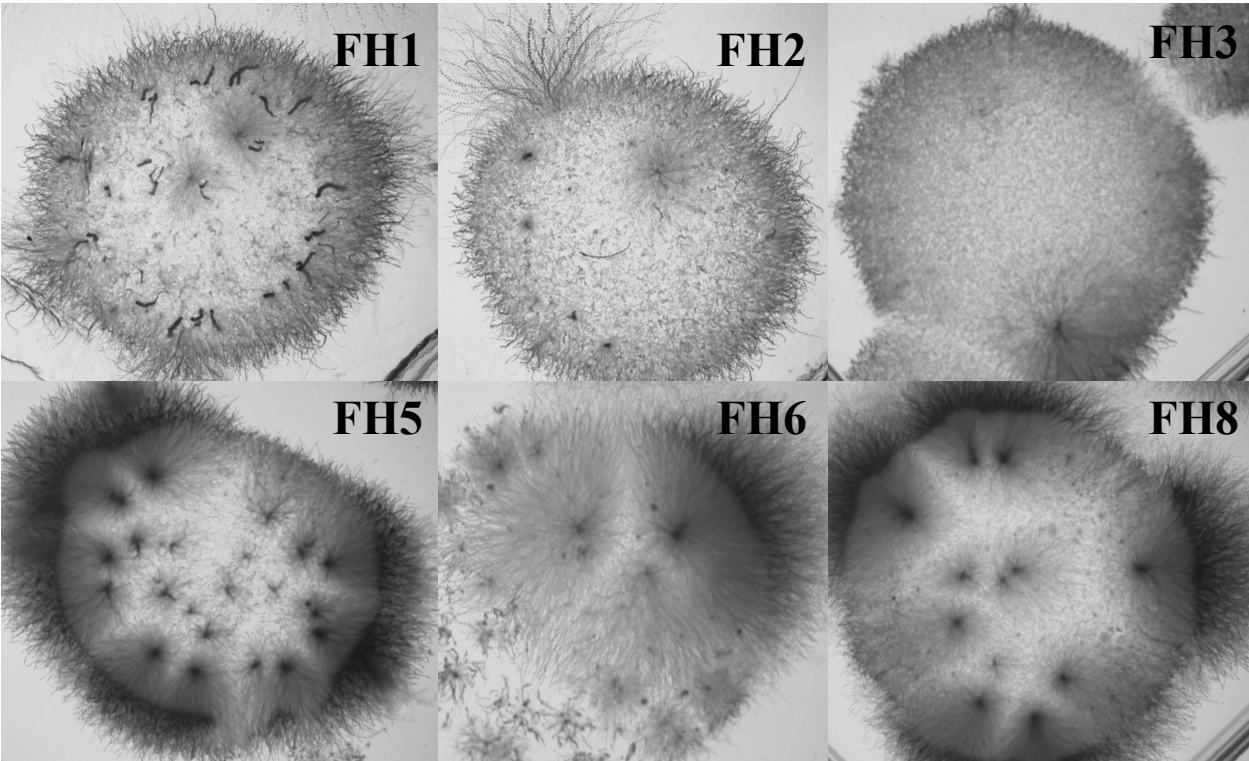
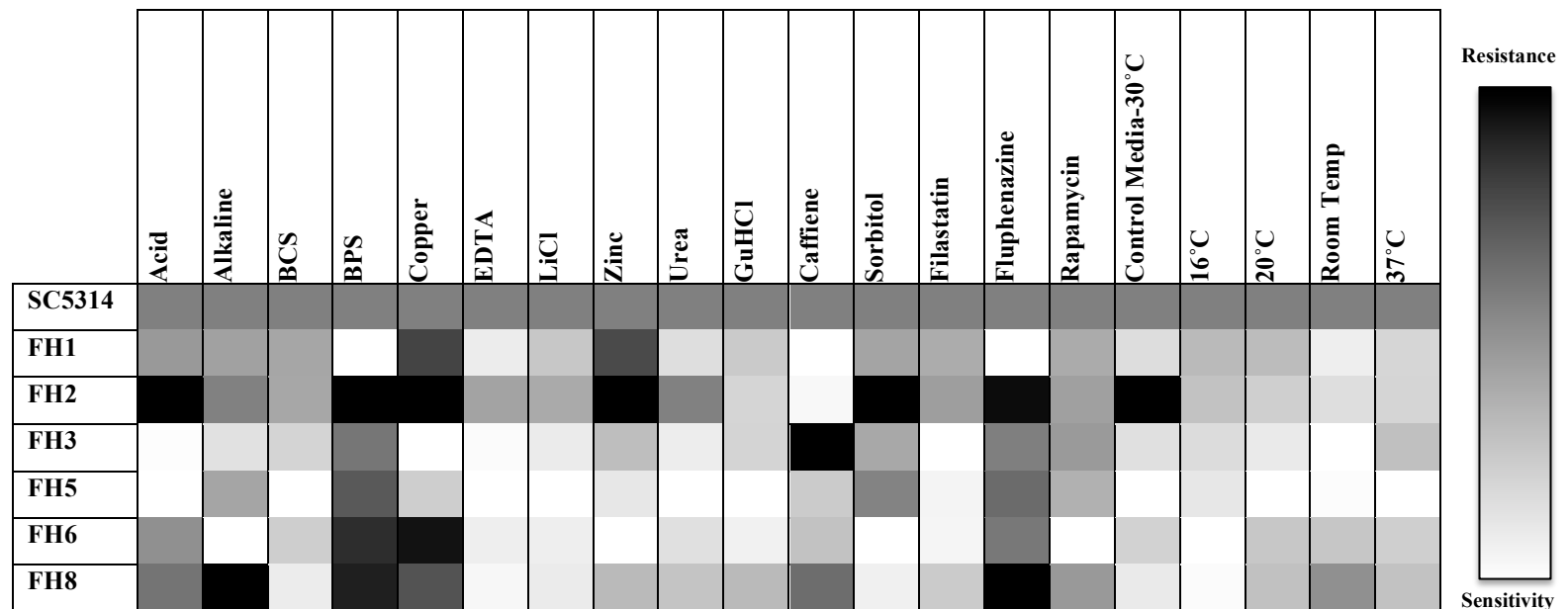
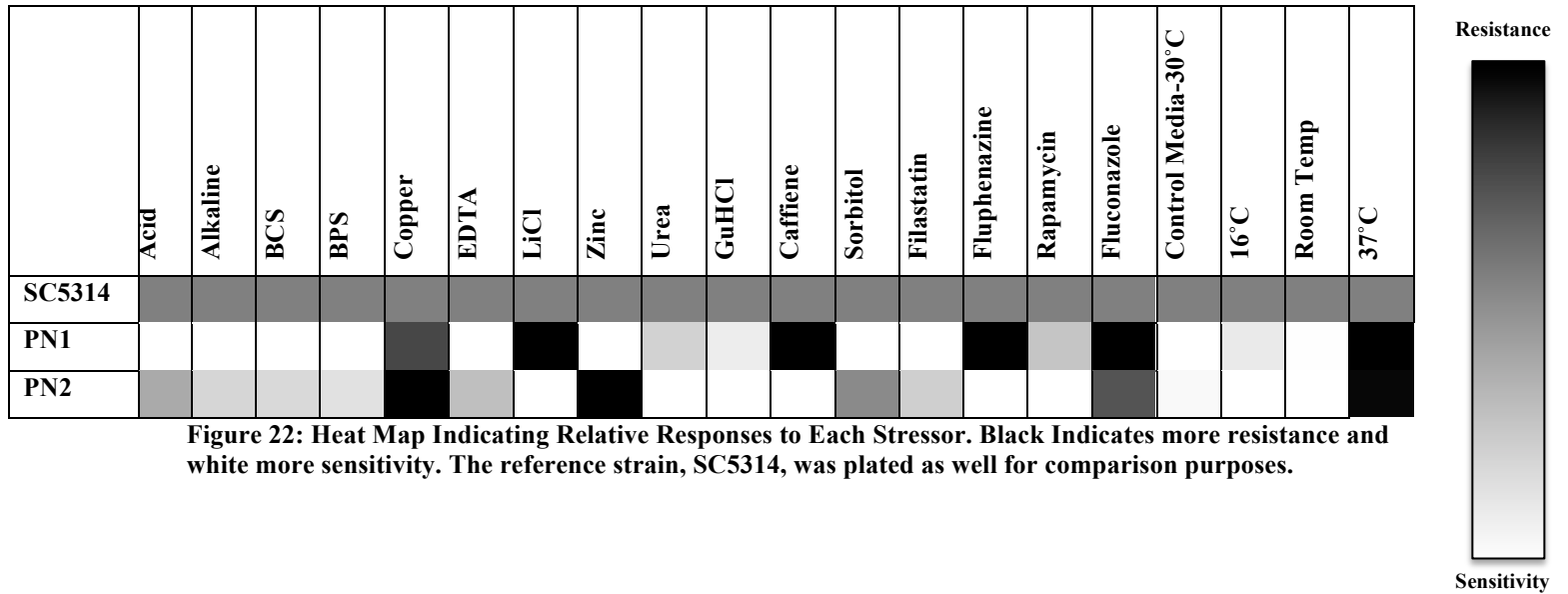


Figure 21: Filamentation Induced by Invasion Assay on YPD Soft Agar Plates of the FH Series. Samples grown at 30°C for 10 days.

Figure 22 shows a heat map produced by comparing the colonies formed (SC5314, PN1, and PN2) on the plate under stress conditions such as acid/base, metal, drug, or temperature. The darker grey or black, indicates that a strain was more resistant (or able to grow unabated) to the condition while the white indicates that the strain was susceptible (or exhibited less growth) under that condition. It is interesting to note that there are several conditions where PN2 is more resistant to a particular condition. Having been isolated from the mouth, and exposed to several changes in environment, it is expected that this commensal strain would be more resistant to such conditions as acid, base, and cooler temperatures. PN1, unfortunately for the patient, is more resistant to the drugs Fluconazole, Fluphenazine, and Rapamycin.

The same type of heat map was created for the FH series. Figure 23 shows that FH2 is often more resistant to the *in vitro* stressors. From this heat map, it can be inferred that the individual infections of this patient respond differently to the stressors, which may be an indicator that methods of prescreening are needed prior to administering drugs. For instance, shown in Figure 23, the patient's infection when FH6 developed may have been more responsive to Rapamycin than any of the other drugs. Additionally, the other strains may not have responded as well to

this treatment. If the infections cannot be phenotypically profiled in some manner, based on these heat maps, a cocktails of drugs, rather than a single drug would be a more effective treatment providing that the patient can tolerate it.



Discussion

A series of phenotyping assays was performed on two clinical isolate series. The series were collected in a time course from two patients with active infections. Patient V (Table 3), a name randomly assigned for anonymity of the patient, was otherwise healthy but was plagued with chronic vaginitis, which affects up to 75 percent of women at some point during their lifetimes (Hong et al., 2014). PN1 was isolated from the active infection, and PN2 was taken from a cheek swab while no infection was present, also known as a commensal strain. This patient was treated with Fluconazole, the first line of antifungal treatments. On the other hand, the FH series was isolated from a patient (Patient B, Table 3) who was immunocompromised from a bone marrow transplant. This patient contracted an invasive *Candida* infection from the transplant and was treated with Fluconazole as well (FH1 and FH2 were collected before treatment began) (Abbey et al., 2014). The information from the host could prove useful in making interspecific connections between series.

The results of the phenotyping assays in this study show, of the PN series, that PN1 is the most virulent. This can be seen in the *in vivo* assays, both Dar and survival (Figures 14 and 15), the *ex vivo* assay (Figure 17), and the *in vitro* adhesion assay (Figure 13). Interestingly, PN1 shows little filamentation (Figure 18) and no invasion into agar (Figure 19), which means that when it was isolated from the patient it was in the yeast cell form. Virulence has been linked to the ability of *C. albicans* to switch between cellular and hyphal forms, and those that switch are more virulent. From this study alone, it cannot be proven that *in vivo*, PN1 is not switching to the hyphal form. It is interesting to correlate the yeast cell form with the mucosal infection though, as the cells do not need to invade the organs. The commensal strain, PN2, showed filamentation (Figure 18) and invasion (Figure 19), which could indicate that the commensal strains are actively working to invade the bloodstream and become active infection. This cannot be proven from this study alone, but more work analyzing differences between infectious and commensal strains is necessary. Additionally, it may be possible that PN1 has suffered a fitness cost for being Fluconazole resistant. That is, PN1 has given up the ability to filament in order to possess this advantage of Fluconazole resistance (Selmecki et al., 2010).

The FH is not as clear-cut as the PN series in terms of which strain is the most virulent. This could be because the patient from whom the strains were isolated was immunocompromised, and therefore the strains were not required to be as virulent. The *in vivo* tests, Dar (Figure 14)

and survival (Figure 16), showed little difference between the majority of the strains. While it appears that there is a difference between FH3 and all other strains (except FH6) in the *ex vivo*, macrophage assay. According to the filamentation assay (Figure 20), the strains that were isolated from fecal samples, which would indicate infection of the gut, showed less filamentation than those isolated from blood samples, indicating invasive infections. This result is also connected to Figure 21, the invasion of the soft agar. It can be seen from these assays that within a single patient, there is no uniform phenotype for *Candida* infections, thus it is unlikely that each new infection would respond to the same drug.

The *in vitro* plate assays of stress conditions could provide insight into possibilities of screening for treatment for each individual infection. Because there was no clear pattern among this clinical isolate series, it is clear that each infection should be treated as a unique infection. New technologies utilizing 96-well formats (Shea et al., 2012) for phenotyping assays could prove useful for quickly and accurately deciding which treatment to administer. For the FH series, FH2, showed resistance to acidic conditions, thus a more basic drug might be considered first, while FH3 and FH5 are more susceptible to acid, and thus may respond to acidic drugs better (Figure 23). FH2 and FH8 are resistant to the drug Fluphenazine, which indicates it would not have been a good treatment; FH1, however, is more susceptible, and thus may have been a good choice for the initial treatment (Figure 23). Additionally, FH6 is susceptible to Rapamycin, the original antifungal antibiotic, but it is now used in transplants for its immunosuppressive effects (Sehgal et al., 1975). An interesting and novel result is that FH3 is susceptible to Filastatin, a new drug affecting filamentation and adhesion (Figure 23) (Fazly et al., 2013). FH3 showed increased adhesion to plastics in the first, *in vitro* assay of this phenomics study (Figure 13), indicating that Filastatin may be a useful treatment at the bedside.

Because there has been a significant increase in Fluconazole resistant *C. albicans* infections, more drugs are needed to fight infection (Control, 2013). In addition to potentially using a new method of prescreening, described above, or cocktails of drugs, rather than the go-to drug, Fluconazole, new drugs, like Filastatin, will need to be discovered or developed.

Chapter 4: *A Published Review*

Pathogens 2014, 3(3), 549-562; doi:[10.3390/pathogens3030549](https://doi.org/10.3390/pathogens3030549)

Host Pathogen Relations: Exploring Animal Models for Fungal Pathogens

Catherine G. Harwood and Reeta P. Rao

Received: 8 April 2014; in revised form: 18 June 2014 / Accepted: 23 June 2014 / Published: 30 June 2014

Abstract: Pathogenic fungi cause superficial infections but pose a significant public health risk when infections spread to deeper tissues, such as the lung. Within the last three decades, fungi have been identified as the leading cause of nosocomial infections making them the focus of research. This review outlines the model systems such as the mouse, zebrafish larvae, flies, and nematodes, as well as *ex vivo* and *in vitro* systems available to study common fungal pathogens.

Keywords: fungal pathogens; *Candida*; *Cryptococcus*; *Histoplasma*; *Aspergillus*; model host systems

1. Introduction

Fungi are ubiquitous and can grow in the mucous membranes and intestinal tracts and on the skin. They are also found in the soil and on plants, trees, and other vegetation. Although not all fungi are pathogenic, some can cause serious disease and pose a significant public health risk. Within the last three decades, fungi have been identified as the leading cause of nosocomial infections (Pfaller, 2007; Prevention, 2014c) especially among immunocompromised patients. This review first outlines the host systems available to study some of the common fungal pathogens, of the genera *Candida*, *Cryptococcus*, *Histoplasma*, and *Aspergillus* (Pfaller, 2007) (Figure 1).

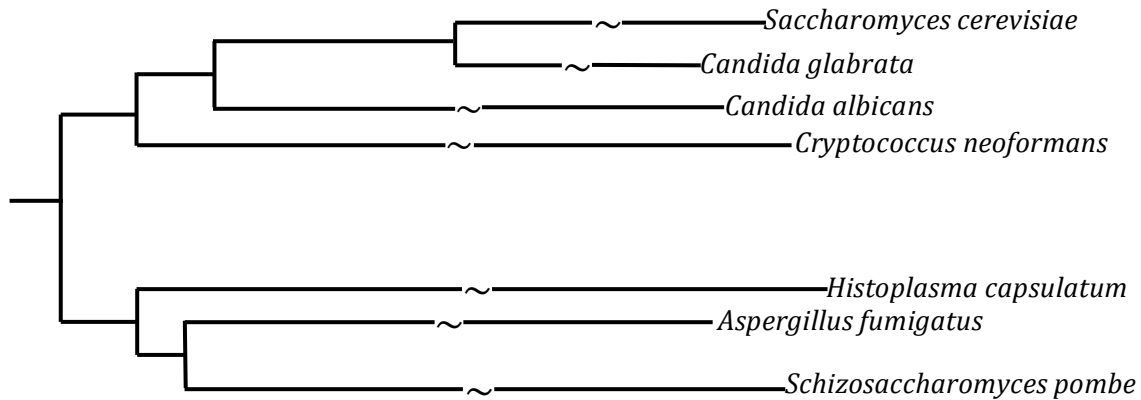


Figure 1: Relative relatedness of the genera discussed in this paper. *S. cerevisiae* and *S. pombe* are used as references for comparison. The arm lengths on the phylogenetic tree are representative and not actual evolutionary distances.

1.1 *Candida*

Yeasts that belong to the genus *Candida* can cause both superficial and invasive infections. Superficial infections include oropharyngeal infection or “thrush,” vaginitis (commonly called “yeast infection”), and diaper rash. While superficial infections are often persistent, they are usually not life threatening. However, when *Candida* invades the bloodstream, the infection becomes systemic and is often deadly (Control, 2013; Prevention, 2014b). Fungi in the *Candida* genus have emerged as major human pathogens, becoming the fourth leading cause of bloodstream infection (BSI) in hospitals around the United States, with 7,000–28,000 annual reports of BSI with a *Candida* (Pfaller, 2007). Some strains, specifically *C. albicans*, are becoming increasingly resistant to conventional antifungal treatments (Pfaller, 2007). For example, in 2013 the United States Center for Disease Control (CDC) reported that fluconazole resistant *Candida albicans* poses a serious threat and is responsible for approximately 3,400 cases annually, including those that are superficial as well as those in the bloodstream (Control, 2013). The lifestyle and virulence strategies used by *C. albicans* are the subject of intense research (Pfaller, 2007). A BSI often begins with a biofilm on medical devices, such as dental implants, catheters, heart valves, bypass grafts, ocular lenses, artificial joints, and central nervous system (CNS) shunts (Prevention, 2014c). In persons whose gastrointestinal tract is heavily colonized by *C. albicans*, it is thought to invade the epithelium in the villi and cross into

the bloodstream. The most common non-*albicans* infections seen are caused by the emerging opportunistic pathogens *C. parapsilosis*, *C. tropicalis*, and *C. glabrata*.

Candida parapsilosis is also capable of forming biofilms on catheters, which can lead to systemic infection if the catheter is placed before removing the yeast (Prevention, 2014c). *Candida glabrata*, evolutionarily a distant relative of *C. albicans*, was once considered nonpathogenic (Prevention, 2014c). With the increasing incidence of AIDS and corresponding rise in the use of immunosuppressive agents, *C. glabrata* infections have also increased. *C. glabrata* is the second or third most common causative agent of superficial and systemic *Candida* infections. It is often difficult to treat because it is resistant to many azole antifungal agents (Fidel, 1999). *Candida tropicalis* is the fourth most common species of the *Candida* genus (Pfaller, 2007). It is common among patients with hematologic malignancies. It is sensitive to azole drugs and other antifungal agents, which have decreased the incidence of *C. tropicalis* within the United States. However, worldwide, its incidence continues to rise, which makes it a candidate for study (Pfaller, 2007).

1.2 *Cryptococcus*

There are approximately thirty species of *Cryptococcus*, the most prevalent pathogen being *C. neoformans*. *Cryptococcus neoformans* can be found in soil throughout the world. Humans become infected by inhaling microscopic spores, which can cause mild symptoms to serious lung infections (Prevention, 2014a). *C. neoformans* is also responsible for cryptococcal meningoencephalitis, which occurs in immunocompromised individuals. It can be found worldwide and is commonly fatal in sub-Saharan Africa (Price, 2011). *Cryptococcus gattii*, a lesser known species of *Cryptococcus*, can infect immunocompetent hosts and is found most prominently in tropical and subtropical areas. However, in 1999, there was an outbreak of *C. gattii* on Vancouver Island, Canada. This geographic expansion in its range has resulted in intense epidemiological studies (Fraser, 2005).

1.3 *Histoplasma*

Histoplasmosis, caused by the fungus *Histoplasma capsulatum*, is a rare infection but is important to study because of its wide host range, typically mammals. *Histoplasma capsulatum*

is thought to enter a latent stage that can be reactivated to active histoplasmosis when the patient has a weakened immune system (Rappleye, 2004) even several years post-exposure. Found in the environments most commonly associated with bird and bat droppings where nitrate content is high, *H. capsulatum* lung infections on inhalation of airborne spores, which produces pneumonia-like symptoms (Prevention, 2014d).

1.4 *Aspergillus*

The genus *Aspergillus* is a fungi common in the environment because the spores are aerosolized. Unlike healthy individuals, who are able to expel the spores from their airways, immunocompromised individuals are unable to, which can lead to serious infection, initially in the lungs and then spreading to almost any organ. The two species that are most commonly associated with disease are *A. fumigatus* and *A. flavus* (Willger, 2008). During infection, *A. fumigatus* causes significant inflammation and necrosis of the lung tissue through hyphal growth, restricting oxygen availability in the tissue (Hedayati, 2007). *A. flavus* is the second leading cause of invasive aspergillosis and the most common for superficial infections. For reasons that are unclear, in certain hospitals it is more common in the air than *A. fumigatus* (Rappleye, 2004).

2. Animal Models

Several animal hosts have been used to study fungi that cause these common infections (Figure 2). Each model has its limitations, but can also yield useful information. Therefore, it is crucial that researchers choose an appropriate model best suited to address the experimental hypothesis being tested. The most common host systems are mice, zebrafish larvae, fruit flies, and nematodes.

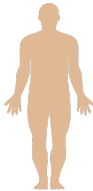

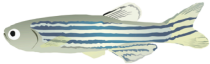




		BENEFITS	LIMITATIONS	
ANIMAL MODELS		 Human	Clinical samples from patients with active infection Hypothesis free experiments	Purifying selection when cultured in laboratory IRB needed Not experimental host Hypothesis generated need to be tested in model host
	Vertebrate	 Mouse	Several modes of infection BSI Oral Vaginal Mammalian immune system	Expensive Handling of individual animals Testing hypothesis is not trivial Overwhelm the immune system Small sample size
		<i>In vivo</i>	 Zebrafish	Vertebrate model Primitive phagocytes present Experimentally tractable
	Invertebrate	 Fruit fly	Primitive phagocytes present Experimentally tractable	Maintain live animals Handling of individual animals Dosage not controlled for oral feeding Wild type fly resistant to infection
			 Nematode	High-throughput applications Experimentally tractable Large sample size Innate immune pathways conserved Can be frozen indefinitely
OTHER MODELS	<i>Ex vivo</i>	 Cell culture	Primary phagocytes Immortalized phagocytes High-throughput screening	Complex biology of whole organism is ignored Similar to <i>in vivo</i> but not physiological Experimental tools in development
	<i>In vitro</i>	 No host	Phenotypic characterization Morphology Drug sensitivity Biofilm formation Competitive fitness	Not physiological

Figure 2: Summary of various model hosts used to study fungal pathogens

2.1 *Mus Musculus*

The murine model for infection is well developed because of its direct implication for human systems. The mouse has been used to model oral, vaginal, and systemic infections that have been shown to mimic human infection (Conti, 2009; Fidel, 1996; Takakura, 2003).

Approximately 90 percent of HIV and AIDS patients experience an episode of oropharyngeal candidiasis or “thrush.” Rabbits and rats have also been used to model oral infections, but these animal models did not accurately mimic local symptoms of oral infection in humans (Takakura, 2003). A murine model showed typical lesions, associated with disease, allowing for more accurate quantification of the disease burden (Conti, 2009). This model for oral *Candida* infection has significantly contributed to our understanding of the disease (Jr, 2002; Koh et al., 2008; Kumamoto and Vinces, 2005a). For example, it has been used to show that Th17 helper T-cells and their secreted cytokine IL-17 have a protective role against oral candidiasis. Oral candidiasis can lead directly to deep tissue (esophageal or stomach) or systemic *Candida* infections (Thewes, 2007).

Recurring vulvovaginitis, which affects approximately five to ten percent of healthy women of childbearing age, is primarily caused by *C. albicans* or *C. glabrata*. A murine model to understand the effects of vaginitis has been developed (Wormley, 2001). Women with diabetes are particularly at risk for developing vaginitis. This is an important correlation between vulvovaginitis and *Candida* strains, which was used to validate this model. A diabetic mouse model was more susceptible to *C. glabrata* vaginal infections. Greater than 85 percent of mice showed organisms in lavage fluid and a 25 percent mortality rate by day 10 (Fidel, 1999).

Introducing fungi directly into the tail vein of mice, mimicking a BSI, is widely used (Ikeda, 2000; Lopez-Berestein et al., 1984) and is considered “the Gold Standard” in the field. This model is used to verify genetic determinants of virulence that have been identified using alternate methods. It is also useful for testing the efficacy of antifungal therapies. Because of resistance, new antifungals are in high demand. In order to model antifungal resistance in mammals, venous tail injection of *Candida* strains including *albicans* and *tropicalis* as well as *Aspergillus fumigatus* have been used. The murine model allows for multiple controlled doses of the antifungals (Ikeda, 2000).

While the mouse is the smallest mammal that mimics many fungal diseases of humans, the model has serious limitations. These include: ethical considerations that prohibit testing on large

numbers of animals; the small sample size (n) makes it challenging to observe small differences; the fungal burden introduced in the bloodstream via the tail vein can overwhelm the immune system of the mouse, while lower fungal burdens escape detection or do not yield statistically reproducible results; the mouse is also not experimentally tractable for hypothesis-driven research; lastly, knockouts are expensive, time consuming, and laborious. Therefore, to test mechanistic hypotheses involving multiple genes, other experimentally tractable facile models such as zebrafish, fruit flies, and nematodes, are used.

2.2 Zebrafish

Zebrafish have been used extensively to study developmental biology (van der Sar et al., 2004). Recently, they have been used as vertebrate model hosts to study the interface between a fungal pathogen and the host immune system. Zebrafish express cytokines, macrophages, neutrophils, dendritic cells, mast cells, eosinophil, T-cells, and B-cells that are evolutionarily related to those of humans (Tobin, 2012). Phagocytes are the primary line of defense against fungal infections. In defense, *C. albicans* has been shown to hyphae that can escape the phagosomes (Liu et al., 1994; Lo, 1997; Lorenz et al., 2004).

Phagocytes, neutrophils, and macrophages, ingest the fungi and inactivate, via multiple mechanisms, including reactive oxygen species (Jain, 2013; Jain et al., 2009) and reactive nitrogen species (Németh). Patients with neutropenia or defects in NADPH oxidase present an increase in infections with *C. albicans* (Lopez-Berestein et al., 1984; Robbins et al., 2010).

Zebrafish larvae are transparent, and therefore, dissemination of the infection can be microscopically tracked (Brothers, 2011) offering a unique perspective compared to adult fish. Furthermore, larval innate immunity can be efficiently modulated using antisense morpholino mediated gene knockdown (Summerton and WELLER, 1997).

The dimorphic transition between hyphal and yeast form cells is an important virulence determinant for *C. albicans*. The *tup1* mutant of *C. albicans* is locked in a filamentous form and is avirulent in a murine model (Braun and Johnson, 1997). As a corollary, the *cph1efg1* null mutant of *C. albicans* is restricted to yeast form cells under most conditions (Kumamoto and Vices, 2005b; Rao et al., 2010), due to mutations in the master regulator of hyphal growth. This mutant has been shown to be less virulent in mice, fruit flies, and nematodes (Brennan, 2002; Chamilos, 2006; Pukkila-Worley et al., 2011). Zebrafish were exposed to the *cph1efg1*

mutant as a test of virulence. Using fluorescent imaging in the transparent larvae, the non-hyphal forming mutant strain was shown to be less virulent in zebrafish larvae (Brennan, 2002). Imaging the macrophages and neutrophils infected with *C. albicans* gave an *in vivo* view of phagocytosed *C. albicans* surviving and/or dividing. This *in vivo* evidence leads to the conclusion that production of reactive oxygen species by the phagocyte's NADPH oxidase, which has previously been implicated in mice and nematodes (Chávez et al., 2007; Frohner et al., 2009), also provides resistance to *C. albicans* in zebrafish (Brothers, 2011).

While zebrafish are a smaller vertebrate alternative to the murine model, it has certain limitations. Like the mouse, propagation of the fish requires a substantial capital investment for a facility and the personnel to maintain them. Furthermore, zebrafish are typically infected via microscopic injection that requires handling of individual animals, and is thus labor intensive.

2.3 *Drosophila Melanogaster*

Drosophila melanogaster is a well-developed experimental system used to model many aspects of biology (Kornberg and Krasnow, 2000). It has a short life cycle and is easy to maintain and manipulate with a large collection of mutant lines. Used as a host for gram-positive and negative bacteria (Leclerc and Reichhart, 2004) and more recently, fungi (Alarco et al., 2004), *D. melanogaster* immunity has been shown to possess extensive conservation with mammalian innate immunity pathways, which make it a strong model system. *Drosophila* hemocytes mimic phagocytes in vertebrates, but they lack an acquired immune system. The *D. melanogaster* innate immune response is characterized by the production and release of stable antimicrobial peptides by the fat body.

Direct injection of the fungal pathogen into the hemolymph results in a systemic infection and allows for precise calculation of fungal burden. Wild type flies are able to contain a systemic infection but unable to kill injected yeast. Flies with a mutation in the toll pathway succumb to systemic fungal infections. This immunodeficient fly model has been used as a host for the study of infectious agents (Glittenberg, 2011; Leclerc and Reichhart, 2004; Lemaitre et al., 1996; Quintin et al., 2013).

The infectious agent can also be introduced into the normal *Drosophila* diet, although there is no way to accurately monitor intake (Chamilos, 2006). The feeding protocol is amenable to

scale-up studies for unbiased mutant screening to uncover novel virulence mechanisms. In addition, antifungal agents can be mixed in with their normal diet for studies of drug efficacy.

2.4 *Caenorhabditis Elegans*

Like *D. melanogaster*, the nematode, *Caenorhabditis elegans*, has been used extensively as a model system to study various biological phenomena, due to many positive aspects including a rapid lifecycle, its completely sequenced genome, genetically identical progeny (due to self-fertilization), and a transparent cuticle that facilitates whole animal microscopy (Stiernagle, 2006). More recently, it has been used as an animal model for the study of infectious disease (Ewbank, 2002; Garsin et al., 2003; Hodgkin, 2000; Jain, 2013). Nematodes are exposed to the infectious agent in their diet, therefore multiplicity of infection is not easily determined (Mylonakis, 2002). Fungi concentrate distally to the pharyngeal grinder and infected worms show a distended gastrointestinal system (Jain, 2013; Jain et al., 2009; Mylonakis, 2002).

Caenorhabditis elegans has been a host model for many gram-positive and gram-negative bacterial infections such as *Salmonella typhimurium*, *Pseudomonas aeruginosa*, and *Staphylococcus aureus*. Certain long-lived *C. elegans* mutants show immunity to these bacterial infections (Mahajan-Miklos, 1999). Recently, *C. elegans* was used as a host to study fungal diseases, but more importantly discoveries made in worms recapitulate virulence patterns in mouse and human infection (Mylonakis, 2002). For example, several virulence genes, including protein kinase A (PKA), protein kinase R (PKR), and G-protein alpha (GPA) were first identified in *C. neoformans*, which modulates virulence in *C. elegans* (Mylonakis et al., 2004). These same genes were later shown to be important for *Cryptococcus* infection in mammals (Mylonakis, 2002). Disrupting PKA increases virulence of *C. neoformans* in mice (D'Souza et al., 2001), a phenomenon that was replicated in *C. elegans*.

Infected nematodes show a deformity in the post-anal region (Dieterich et al.), which is visible four- to five-days post-infection (Hodgkin, 2000; Jain, 2013). Other disease markers such as swelling in the vulvar region and intestinal distention have been reported for both fungal and bacterial infections (Hodgkin, 2000; Jain, 2013). Ingestion of yeast can be microscopically monitored over time using fluorescently marked *C. albicans* (Jain, 2013), confirming that accumulation of fungi is the likely cause of intestinal distension.

These disease markers can be used to study the progression of disease, while survival assays provide a quantitative measure of disease and death. As a simple starting model, *C. elegans* is a quick and inexpensive way to study virulence of many fungal species. However, like *D. melanogaster*, the results often need to be verified in a mammalian system, like mice.

The nematode is a convenient model especially to study innate immunity since facets of its innate immune system are conserved in humans (Jain, 2013; Jain et al., 2009) and host genes can be easily modulated via RNAi (Kim and Rossi, 2008). Furthermore, infections do not require handling of animals and, therefore, can be performed in a high throughput fashion. Another advantage is that worms can be frozen (indefinitely) and thus do not require maintenance of live cultures.

Nematodes, however, cannot be propagated at the human body temperature of 37° C. Therefore, the larvae of the greater wax moth *Galleria mellonella* are used to study virulence at 37° C. Specifically, the virulence of certain clinical isolates of *C. albicans* has been correlated between the *G. mellonella* infections and murine models, lending credibility to the system. In addition, several bacterial strains, such as *Pseudomonas aeruginosa*, have been tested in the moth system. In contrast to other readily available, inexpensive systems, like *D. melanogaster* and *C. elegans*, *G. mellonella* has to be tediously injected one at a time and its genome has not been sequenced, which makes knockouts and other genetic manipulations more difficult (Brennan, 2002).

3. Ex Vivo Systems

Ex vivo systems for studying fungal infections include phagocytes in culture and tissue explants, as shown in Figure 2. Phagocytes are our primary defense against fungal pathogens. Macrophages and neutrophils play a central role in antifungal immunity by ingesting and killing pathogens (Lo, 1997; Lorenz and Fink, 2001; Rubin-Bejerano et al., 2003; Wheeler and Fink, 2006). They are also responsible for initiating adaptive immune responses.

Cultured macrophages can include both primary and immortalized cells. Immortalized cell lines such as the RAW264.7 and J774 are robust and can withstand harsh treatments such as trypsinization and scraping while still proliferating. Immortalized macrophages have been instrumental in uncovering aspects of *Candida* virulence such as hyphae formation, extracellular lipase, and proteinase production (Németh, 2013). However, the multiple passages

and harsh growth and handling conditions of immortalized macrophages specifically select them to be more robust at the expense of other properties that might be important for immunity. Therefore, primary macrophages are considered better than immortalized macrophages even though they are more difficult to extract and maintain (Németh, 2013).

Németh, *et al.* infected both immortalized murine macrophage and primary human macrophage hosts with *Candida parapsilosis* in the paper “Characterization of Virulence Properties in the *C. parapsilosis Sensu Lato* Species” (Németh, 2013). The fungi exhibited varying degrees of virulence when exposed to each type of macrophage (Németh, 2013). *C. parapsilosis* exhibited the highest resistance to killing by primary human macrophages, compared to *C. orthopsilosis* and *C. metapsilosis*. However, this difference was not reflected in the murine virulence model. In spite of these differences, cultured cell lines are useful and can complement live, whole-animal studies.

Transcriptional profiling of *C. albicans* within phagosomes has been performed (Thewes, 2007). Strains have been shown to quickly adapt and alter their transcriptional profile in many circumstances related to infection, such as response to stress, iron deprivation, and interaction with macrophages. In order to understand *Candida* infection, Thewes, *et al.* used *in vivo* and *ex vivo* techniques to understand the genes associated with infection in parenchymal organs (e.g., liver). For example, an *ex vivo* tissue explant of porcine liver-infected tissue was shown to mimic murine model of *in vivo* infection (Thewes, 2007). *Candida albicans* was directly injected into both mice and pig livers. *Ex vivo* tissue explants from both exhibited a similar extent of deep tissue invasion (Thewes, 2007). Excised murine vaginal mucosal tissue is also used as a substrate to study vaginal infections (Harriott *et al.*, 2010). These *ex vivo* systems provide a simple and rapid method for optimizing conditions prior to *in vivo* assays (Fazly *et al.*, 2013).

4. In Vitro Systems

Viewing a fungal phenotype on an agar plate is a “host-free” method to study fungal virulence. For example, *C. albicans* mutants such as *efg1*^{-/-} and *cph1*^{-/-} showed reduced hyphal growth on agar media, and the double knockout *efg1*^{-/-} *cph1*^{-/-} does not form hyphae under most *in vitro* conditions. This double knockout mutant was later shown to be avirulent in a murine model, which linked hyphal growth and virulence (Lo, 1997). Since then, many

mutants with defects in dimorphic transition have been shown to be attenuated in virulence. This *efg1*^{-/-} *cph1*^{-/-} double mutant has been used extensively to validate other host models (Brothers, 2011; Jain, 2013).

Chemical sensitivity *in vitro* can be used as a proxy for pathways that are important *in vivo*. Fungal response to important aspects of the human innate immune system such as reactive oxygen species can be mimicked *in vitro* using menadione and hydrogen peroxide (Homann, 2009). Cell wall stressors such as sodium dodecyl sulfate (SDS), caffeine, and calcofluor (Homann, 2009) have been used *in vitro* to study the effects on the cell wall. Since human cells do not possess cell walls, they are good targets for drugs, like capsosungin (Homann, 2009). Other drug sensitivity assays can be modeled *in vitro* by plating fungi on drug-infused plates (Homann, 2009). The role of metals can be mimicked *in vitro* by using scavengers or chelators *in vitro*. For example, the *C. albicans* transcription factor Hap43 is activated by iron deficiency *in vivo* (Hsu et al., 2011) and is also required for growth upon iron-deprivation *in vitro* (Baek et al., 2008; Homann, 2009; Hsu et al., 2011). Hap43 also regulates virulence, and mice infected with *hap43*^{-/-} strains showed attenuated virulence (Baek et al., 2008). The pathways regulating iron homeostasis are complicated, but *in vitro* techniques may be used to fine tune regulatory networks.

Biofilm formation is a virulence determinant that is well suited to study in a host-free environment. Biofilms are typically made up of multiple microbial communities that stick to each other and are an abiotic surface (Hogan et al., 2004; O'Toole et al., 2000). The microbes secrete extracellular materials (Chandra, 2001) and are important in the context of infection because they are drug resistant. For example, *C. albicans* is thought to gain access to the bloodstream via plastic devices such as central lines, catheters, or other implanted devices. The mortality rate for patients with catheter-related BSI is approximately 41 percent (Chandra, 2001).

Formation of biofilm proceeds in three phases: the early phase where the fungal communities attach to the surface, grow, and aggregate; the intermediate phase where the extracellular matrix, a predominantly noncellular material, covers fungal microcolonies and is secreted into the milieu (Chandra, 2001); (*C. albicans* also transition into the hyphal form); finally, during the maturation phase, the extracellular material grows and planktonic yeast cells bud off and disseminate.

In vitro models can also be used to study reconstituted epithelial cells in order to model human infection (Figure 2). The role of certain virulence-related genes in fungal infection can first be modeled *in vitro* on reconstituted epithelial cells before using more expensive *in vivo* models. For example, the secreted aspartyl proteinases (SAP) of *C. albicans* have been linked to virulence in mucosal infection in clinical isolates of patients with chronic vaginitis (Schaller, 2003). This family of 10 enzymes was first studied using reconstituted vaginal epithelial cells in order to link them to epithelial damage that occurs during disease. The 10 *SAP* genes are differentially expressed during infection. Specifically, *SAP1*, *SAP6*, *SAP9*, and *SAP10* showed a stronger signal in conjunction with mucosal lesions (Schaller, 2003). These *SAP* genes showed strong signals in both *in vitro* models as well as *in vivo* samples from patients with vaginal infections. These lesions showed severe damage in the epithelial cells including: edema, vacuolization, and detachment of keratinocytes. Differential SAP expression has also been linked to “thrush” infections (Schaller, 2003). Despite this, they are not identical to those present in vaginal infections (Schaller, 2003).

In vitro systems are extensively used to study fungal virulence to get mechanistic clues, but often have to be validated in an animal model to account for the complex biology in the host environment. Each of these systems is used to study *Candida* with the hope of finding better methods to treat infections.

5. Conclusions

Several models, including *in vivo*, *ex vivo*, or *in vitro* systems, have been used to study fungal disease. All models have limitations but are useful for generating testable hypotheses. The key is to choose a simple model that can fully address the scientific question being addressed, yet not so simple that the complex and interesting biology is ignored. For example, biofilms and certain drug sensitivities' assays can be first performed *in vitro*, but then must be verified *in vivo*. Simple and inexpensive systems such as *C. elegans* and *D. melanogaster* can unveil the building blocks for infection, which can then be followed up in mammalian systems. Opportunistic fungal infections are increasing in the United States and around the world. It is important that the host system chosen have implications for furthering the knowledge on human-pathogen interactions.

Appendix A: Results of the Initial Screen Designed to Find Mutants that Show an Exaggerated Response to Filastatin

This table shows the compilation of the 233 mutants from the first screen. FAD3 and ORF19.1239 were the only two that showed an increase in adhesion (highlighted in the table).

Table 1: List of mutants pulled out of the initial screen

ORF19.1797	LIP1	LIP10	ORF19.5352	ORF19.1643	ORF19.2446	ORF19.6318	CUP9
ORF19.1162	LSC2	ORF19.3290	IFF6	SPR1	ZCF24	ORF19.4678	ORF19.4843
ORF19.376	SOD6	ORF19.3335	ORF19.4104	DCK1	STE13	SAP3	MNT4
LIP6	ORF19.5547	ORF19.2850	RGS2	SCW4	ZRT1	IFD3	ORF19.3418
ORF19.3611	ORF19.268	PPZ1	STE2	ORF19.2703	CTA9	ORF19.7033	ORF19.7196
ORF19.899	ORF19.2838	ORF19.3874	ORF19.4680	PIN4	YPT7	SIZ1	ORF19.3799
ORF19.100	ORF19.305	ZCF2	HYR3	ARO80	MNN22	YPS7	ORF19.6660
ORF19.215	PRM1	ORF19.2315	ORF19.6348	ORF19.2605	ORF19.3029	ORF19.3453	ORF19.7305
CDG1	SAP8	PCL2	ORF19.557	ORF19.3049	ORF19.7370	CRZ1	RFG1
OPT4	ORF19.255	ORF19.419	KAR3	ORF19.2781	ORF19.3060	ORF19.3488	ORF19.6693
ORF19.6238	ORF19.7516	ORF19.13064	KIC1	RAD18	ORF19.7554	WOR2	ORF19.6245
IFA14	ORF19.192	ORF19.433	SIN3	KAR4	ORF19.3854	ORF19.6293	ORF19.6678
HET1	ORF19.7590	ORF19.50	ORF19.194	CHT2	CAG1	ORF19.4182	ORF19.4292
ORF19.6607	ORF19.8009	ORF19.95	ORF19.199	MUC1	HSL1	ORF19.5892	UGA32
ORF19.5129	ECM14	ORF19.449	BCR1	APM1	ZCF27	ORF19.7381	PIKALPHA
ORF19.698	PGA18	ADP1	ORF19.641	PEX4	ORF19.4350	OPT6	SSU81
OSH3	MNT1	ORF19.2265	TYE7	GRR1	ULP2	KTR4	ORF19.4972
ARL3	ORF19.1573	ORF19.1718	ORF19.2063	ORF19.3982	SGT1	FET3	ORF19.4376
TOS1	ORF19.1576	ORF19.2336	GPA2	PRC2	SWI4	ORF19.4844	ORF19.7086
ORF19.1173	ORF19.1567	ARF3	PDR6	ORF19.4412	CUP2	ORF19.7096	SSK2
SAP7	SAP98	ORF19.1185	YEA4	ORF19.5068	YCP4	MEC3	PTC7
ORF19.757	ORF19.872	CPH2	ORF19.1392	IFA21	ORF19.5291	PEP7	MBP1
ORF19.1219	ORF19.1397	ORF19.1577	KIP2	ENA21	LRO1	ORF19.6526	OCH1
ORF19.782	CHK1	CFL2	ORF19.1411	ERG5	ORF19.5326	STE23	SAP1
ORF19.783	ORF19.3615	KEX2	ORF19.6506	FGR17	RAX1	CIS2	ORF19.6553
ORF19.5247	ECM7	ORF19.5975	ORF19.6802	GAL4	DUR35	IFD6	FAD3
ZCF30	GLO3	ORF19.5644	ORF19.5813	ORF19.5593	SNQ2	ORF19.6802	ORF19.1239
PST3	ECM17	ORF19.5651	RHB1	RBT4	RIM101	AXL1	IFF4
FGR27	TUS1	CLB4	ORF19.7304	FRP1	TOM1	PGA13	ORF19.6653

Appendix B: Results of the Second Screen Designed to Find Targets that Are Blind to the Addition of Filastatin

Table 1 and Table 2 present the results of the second screen. The characterization of each mutant has been provided from the *Candida Genome Database*.

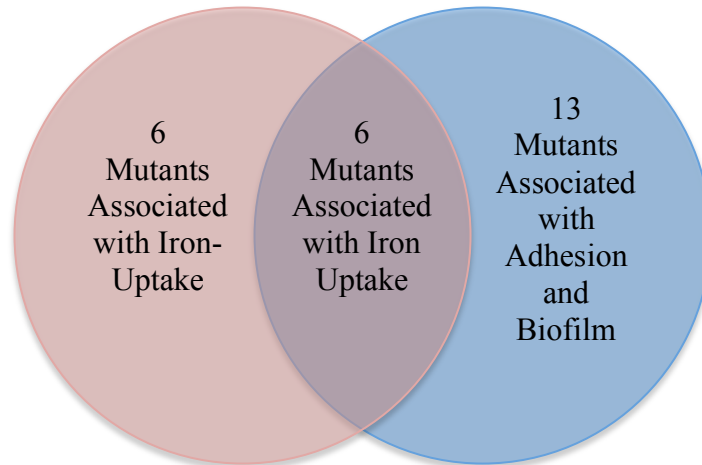


Figure 1: Two Pathways Represented in Second Screen. This figure provides a key for the tables as well.

Table 1: Mutants from the Second Screen that normally adhere more than wild type

Adheres More Than Wild Type	
PRN4	protein with similarity to pirins, flow model biofilm repressed
CSA2	Extracellular-associated protein; repressed by Rim101 at pH 8; regulated by Tsa1, Tsa1B in minimal media at 37 deg; induced by ketoconazole, nitric oxide, Hap43; required for normal RPMI biofilm formation; Bcr1 induced in RPMI
ORF19.3919	RNI-like superfamily domain-containing protein; early-stage flow model biofilm induced; Spider biofilm induced
LIP2	Secreted lipase; member of a differentially expressed lipase gene family; expressed in alimentary tract, but not oral tissue, during mouse oral infection; may have a role in nutrition and/or in creating an acidic microenvironment
RBT5	GPI-linked cell wall protein; hemoglobin utilization; Rfg1, Rim101, Tbf1, Fe regulated; Sfu1, Hog1, Tup1, serum, alkaline pH, antifungal drugs, geldamycin repressed; Hap43 induced; required for RPMI biofilms; Spider biofilm induced
HAK1	Putative potassium transporter; similar to <i>Schwanniomyces occidentalis</i> Hak1p; amphotericin B induced; induced upon phagocytosis by macrophage; Hap43-repressed; rat catheter biofilm repressed
HET1	Putative sphingolipid transfer protein; involved in localization of glucosylceramide which is important for virulence; Spider biofilm repressed
ORF19.6637	Predicted glycosyl hydrolase; hypoxia induced; flow model biofilm induced

HEX1	Beta-N-acetylhexosaminidase/chitinase, highly glycosylated enzyme that is secreted to the periplasm and culture medium; required for full virulence; may have role in carbon or nitrogen scavenging; possibly an essential gene (UAU1 method)
NPR2	Putative urea transporter; induced during infection of murine kidney, compared to growth in vitro; has murine homolog
ORF19.587	Ortholog(s) have transcription export complex localization
ORF19.649	Uncharacterized
CFL11	Protein similar to ferric reductase Fre10p; flucytosine repressed; possibly adherence-induced; possibly an essential gene, disruptants not obtained by UAU1 method; rat catheter biofilm repressed
ORF19.2726	Putative plasma membrane protein; Plc1-regulated; Spider biofilm induced
HYR1	GPI-anchored hyphal cell wall protein; macrophage-induced; repressed by neutrophils; resistance to killing by neutrophils, azoles; regulated by Rfg1, Efg1, Nrg1, Tup1, Cyr1, Bcr1, Hap43; Spider and flow model biofilm induced

Table 2: Mutants from Second Screen that normally adhere less than wild type

Adheres Less Than Wild Type	
ORF19.380	Protein of unknown function; induced by alpha pheromone in SpiderM medium
BTA1	Betaine lipid synthase
ORF19.1365	Putative monooxygenase; mutation confers hypersensitivity to toxic ergosterol analog; constitutive expression independent of MTL or white-opaque status
HWP2	GPI-anchored, glycosylated cell wall protein; required for biofilm formation, adhesion, filamentous growth on some media; expressed in hyphae; mutant delayed in virulence; regulated by Efg1, Tup1; similar to Hwp1 and Rbt1 domains
MTS1	Sphingolipid C9-methyltransferase; catalyzes methylation of the 9th carbon in the long chain base component of glucosylceramides; glucosylceramide biosynthesis is important for virulence; Spider biofilm repressed
FLO9	Putative adhesin-like cell wall mannoprotein; repressed during the mating process; mutation confers hypersensitivity to toxic ergosterol analog; decreased transcription is observed upon fluphenazine treatment
ORF19.5449	Predicted integral membrane protein; Spider biofilm induced
PGA10	GPI anchored membrane protein; utilization of hemin and hemoglobin for Fe in host; Rim101 at ph8/hypoxia/ketoconazole/ciclopirox/hypha-induced; required for RPMI biofilm formation, Bcr1-induced in a/a biofilm; rat catheter biofilm repressed
KRE5	UDP-glucose:glycoprotein glucosyltransferase; 1,6-beta-D-glucan biosynthesis, hyphal growth, virulence in mouse IV model; partially complements <i>S. cerevisiae</i> kre5 mutant defects; flow biofilm repressed, Bcr1-repressed in RPMI a/a biofilms
ORF19.2484	Has domain(s) with predicted peptidase activity and role in proteolysis
GZF3	GATA-type transcription factor; oxidative stress-induced via Cap1; mutant has abnormal colony morphology and altered sensitivity to fluconazole, LiCl, and copper; Spider biofilm induced

ORF19.3108	Putative DNA repair methyltransferase; induced by nitric oxide independent of Yhb1; Spider biofilm induced
ORF19.3226	Ortholog(s) have role in intracellular sterol transport and extracellular region, fungal-type vacuole lumen localization
HYR4	Putative GPI-anchored adhesin-like protein; Rim101-repressed; constitutive expression independent of MTL or white-opaque status
ORF19.3404	Protein of unknown function; transcription repressed by fluphenazine treatment
ORF19.3763	Has domain(s) with predicted serine-type endopeptidase activity and integral to membrane localization
GYP1	Putative Cis-golgi GTPase-activating protein; transcript regulated by Nrg1, Mig1, and Tup1
KIS1	Snf1p complex scaffold protein; similar to <i>S. cerevisiae</i> Gal83p and Sip2p with regions of similarity to Sip1p (ASC and KIS domain); interacts with Snf4p; mutants are hypersensitive to caspofungin and hydrogen peroxide; Hap43p-repressed gene
ORF19.4195	Ortholog of <i>C. dubliniensis</i> CD36 : Cd36_60540, <i>C. parapsilosis</i> CDC317 : CPAR2_602830, <i>Candida tenuis</i> NRRL Y-1498 : CANTEDRAFT_108530 and <i>Debaryomyces hansenii</i> CBS767 : DEHA2F15532g
CAS5	Transcription factor; cell wall damage response; required for adherence, response/resistance to caspofungin; repressed in core stress response; mutants have reduced CFU in mice, hyphal defect in <i>C. elegans</i> infection; Spider biofilm induced
ORF19.4805	Putative membrane protein; induced by alpha pheromone in SpiderM medium; Hap43-induced gene; Spider biofilm induced
IFF11	Secreted protein required for normal cell wall structure and for virulence; member of the IFF family; Hap43p-repressed gene
ORF19.5406	Predicted plasma membrane associated protein phosphatase; required for normal filamentous growth; mRNA binds She3 and is localized to hyphal tips (1)
PTC7	Protein phosphatase, type 2C; has S/T phosphatase activity, Mn ²⁺ /Mg ²⁺ dependent; predicted membrane-spanning segment and mitochondrion-targeting signal

***The descriptions of these genes were found on the Candida Genome Database**

Appendix C: Another View at the Interaction Assay Results

The interaction assay between Filastatin and Hemoglobin shows a decrease in adhesion when Filastatin alone is added, and an increase in adhesion when only Hemoglobin is added. Additionally, when the two are added in equal concentrations, the results show the level of adhesion is not simply the individual effect of each, but some interaction. However, this result alone does not prove what the interaction is.

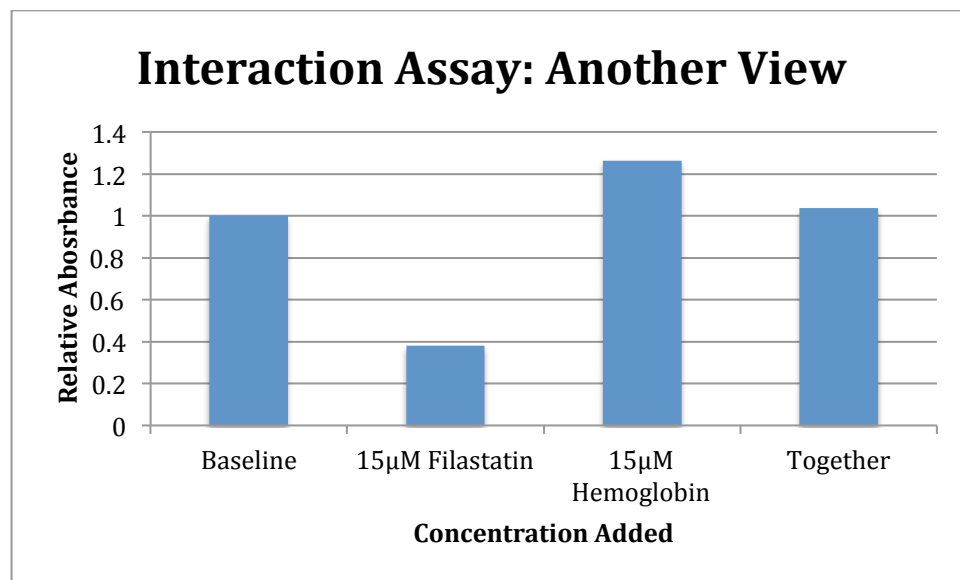


Figure 1: Another View of the Interaction Assay. This graph shows that when the same concentration of both Filastatin and Hemoglobin are added, the results are not simply additive, indicating an interaction.

Appendix D: Summary of Results from Chapter 1

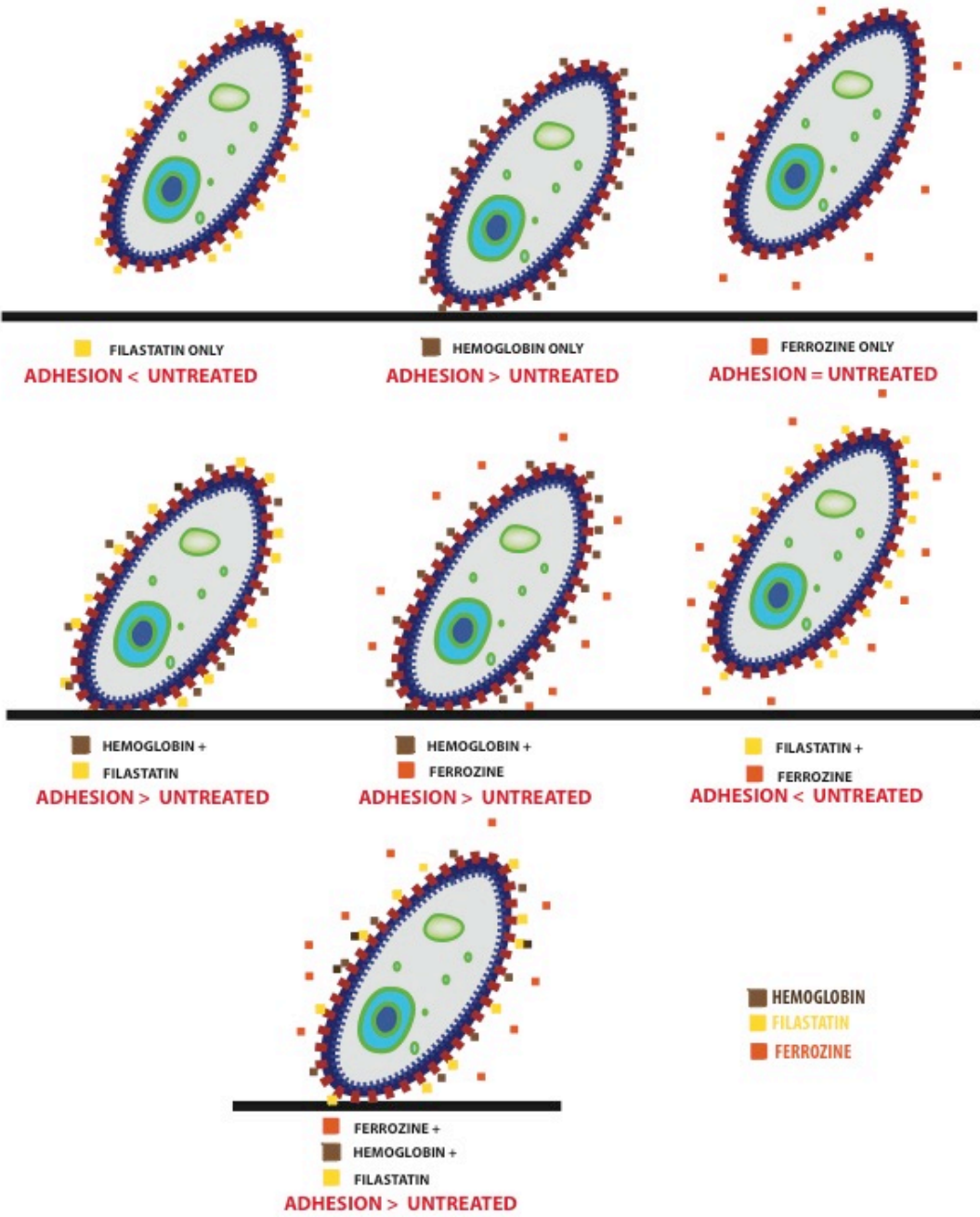


Figure 1: Summary of the Results from Chapter 1, Figure Produced by R.P Rao

Appendix E: Results of the Statistical Analysis on the Survival Assay

Both the Log Rank Test and the Gehan-Breslow Test were performed analyzing the differences between the reference strain and the clinical isolate series and within each clinical isolate series.

Strains Compared	Log Rank Test	Gehan-Breslow Test
SC5314-PN Series	<0.0001	<0.0001
SC5314-FH Series	<0.0001	<0.0001
PN1-PN2	0.0043	0.0068
FH1-FH2	0.1386	0.5688
FH1-FH3	0.8788	0.7111
FH1-FH5	0.1655	0.0692
FH1-FH6	0.3599	0.4255
FH1-FH8	0.7906	1.0000
FH2-FH3	0.0763	0.4672
FH2-FH5	0.0010	0.0040
FH2-FH6	0.5078	0.7770
FH2-FH8	0.0914	0.5063
FH3-FH5	0.2055	0.0647
FH3-FH6	0.4300	0.6560
FH3-FH8	0.5758	0.7297
FH5-FH6	0.1127	0.0156
FH5-FH8	0.9954	0.1282
FH6-FH8	0.2918	0.5795

Appendix F: Phenotypic Examination of a Laboratory Tetraploid Strain

The following figures and tables show the results of the phenotypic profile of the reference strain (SC5314), a laboratory generated tetraploid strain (RBY18), as well as its two parent strains (RBY16 and MMY304). *In vivo*, survival, and several *in vitro* assays have been performed on these strains, though no correlation between phenotype and ploidy could be made.

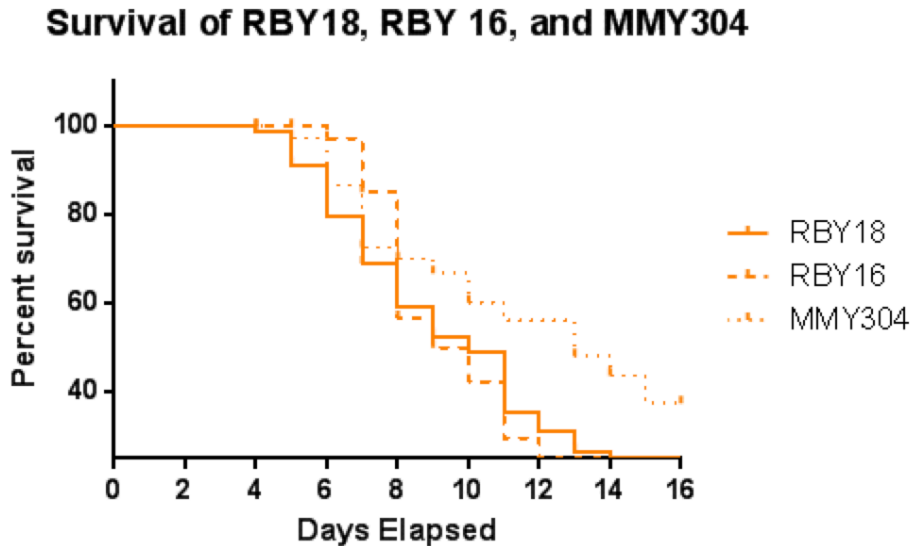


Figure 1: Survival Curves for Laboratory Tetraploid Strain, RBY18, and its two diploid parents, RBY16 and MMY304

Table 1: Reported p values for Log Rank Test and Gehan-Breslow Tests for Survival Data of Clinical Isolates. Significant p values are bolded.

Strains Compared	Log Rank Test	Gehan-Breslow Test
RBY18-RBY16	0.7441	0.1032
RBY18-MMY304	0.0517	0.1006
RBY16-MMY304	0.0805	0.7160

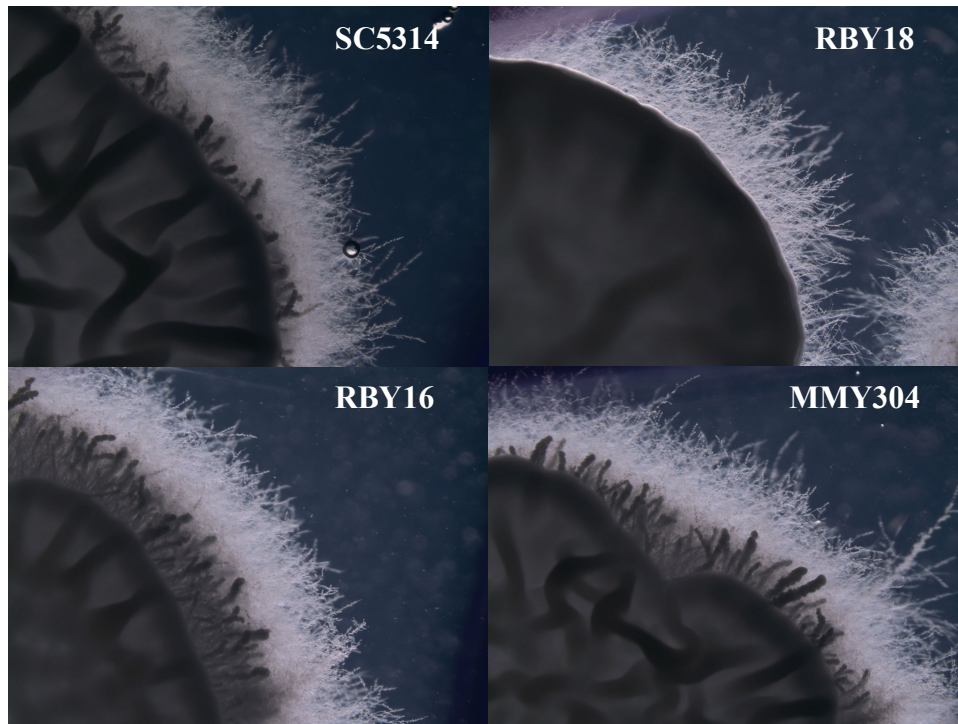


Figure 2: Filamentation on spider media of the reference strain, SC5314, RBY18, RBY16, and MMY304 were included in this study to make potential connections between ploidy and morphology.

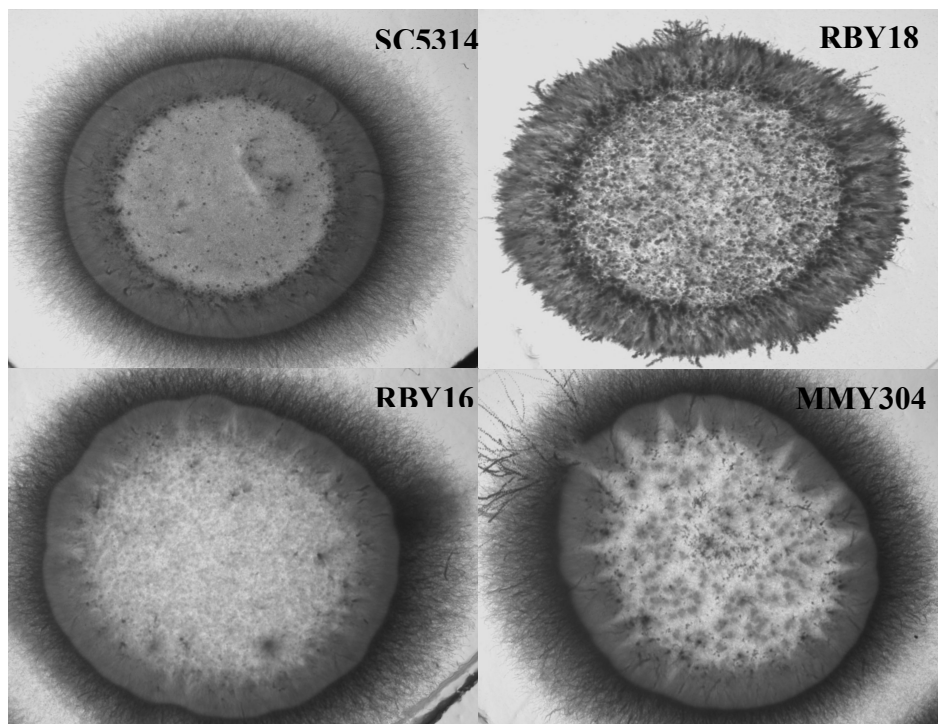


Figure 3: Invasion of Reference Strain, SC5314, and RBY18, RBY16, and MMY304.

	Acid	Alkaline	BCS	BPS	Copper	EDTA	LiCl	Zinc	Urea	GuHCl	Caffeine	Sorbitol	Filastatin	Fluphenazine	Rapamycin	Control Media-30°C	16°C	Room Temp	37°C
SC5314	Grey	Grey	Grey	Grey	Grey	Grey	Grey	Grey	Grey	Grey	Grey	Grey	Grey	Grey	Grey	Grey	Grey	Grey	Grey
RBY18	Grey	Grey	Grey	White	Black	Grey	Black	Black	White	White	Grey	Black	Grey	White	White	Grey	White	Grey	White
RBY16	White	White	Grey	Grey	Black	Grey	Black	Black	White	White	Grey	Black	White	Grey	White	Grey	White	Grey	White
MMY304	Grey	Grey	White	Grey	Black	Black	Grey	Grey	White	White	White	White	White	Black	Grey	Grey	White	White	Grey

Figure 4: Heat Map Indicating Relative Responses to Each Stressor. Black indicated more resistance and white more sensitivity. The reference strain, SC5314, was plated for comparison purposes as well.

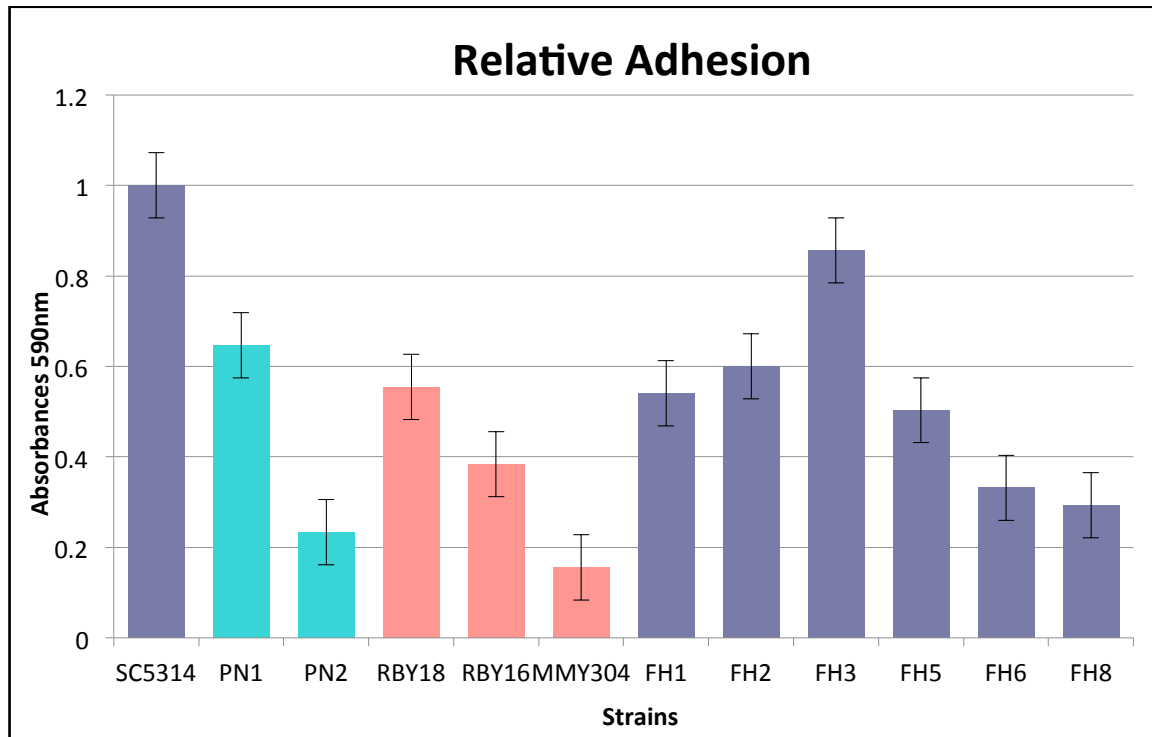


Figure 4: Relative Adhesion of all strains tested compared to the reference strain SC5314. This table includes a lab tetraploid, RBY18, and its two diploid parents, RBY16 and MMY304.

Appendix G: Requirements for Graduation

Academic

M.S. Requirements

	Required credits	Received
BBT courses	3 Classes	4 Classes
Advanced Genetics and Cellular Biology.....		A
Experimental Design and Statistics.....		A
Medical Device Regulation.....		A
Special Topics: Animal Cell Culture Technology.....		B
BB501 Seminar	Every semester	✓
Journal Club	1	1
Ethics	1	1
Research Credits	At least 6	19
Manuscript	No Requirement	1 Review Published

Pathogens **2014**, 3(3), 549-562; doi:[10.3390/pathogens3030549](https://doi.org/10.3390/pathogens3030549)

Thesis

Works Cited

- Abbey, D.A., Funt, J., Lurie-Weinberger, M.N., Thompson, D.A., Regev, A., Myers, C.L., and Berman, J. (2014). YMAP: a pipeline for visualization of copy number variation and loss of heterozygosity in eukaryotic pathogens. *Genome medicine* 6, 1-16.
- Alarco, A.-M., Marcil, A., Chen, J., Suter, B., Thomas, D., and Whiteway, M. (2004). Immune-deficient *Drosophila melanogaster*: a model for the innate immune response to human fungal pathogens. *The Journal of Immunology* 172, 5622-5628.
- Andes, D., Nett, J., Oschel, P., Albrecht, R., Marchillo, K., and Pitula, A. (2004). Development and characterization of an in vivo central venous catheter *Candida albicans* biofilm model. *Infection and immunity* 72, 6023-6031.
- Ariyachet, C., Solis, N.V., Liu, Y., Prasadarao, N.V., Filler, S.G., and McBride, A.E. (2013). SR-like RNA-binding protein Slr1 affects *Candida albicans* filamentation and virulence. *Infection and immunity* 81, 1267-1276.
- Baek, Y.-U., Li, M., and Davis, D.A. (2008). *Candida albicans* ferric reductases are differentially regulated in response to distinct forms of iron limitation by the Rim101 and CBF transcription factors. *Eukaryotic cell* 7, 1168-1179.
- Beyda, N.D., Lewis, R.E., and Garey, K.W. (2012). Echinocandin resistance in *Candida* species: mechanisms of reduced susceptibility and therapeutic approaches. *Annals of Pharmacotherapy* 46, 1086-1096.
- Bliss, J.M., Wong, A.Y., Bhak, G., Laforce-Nesbitt, S.S., Taylor, S., Tan, S., Stoll, B.J., Higgins, R.D., Shankaran, S., and Benjamin, D.K. (2012). *Candida* virulence properties and adverse clinical outcomes in neonatal candidiasis. *The Journal of pediatrics* 161, 441-447. e442.
- Braun, B.R., and Johnson, A.D. (1997). Control of filament formation in *Candida albicans* by the transcriptional repressor TUP1. *Science* 277, 105-109.
- Brennan, M., David Y. Thomas, Malcolm Whiteway, and Kevin Kavanagh (2002). Correlation between virulence of *Candida albicans* mutants in mice and *Galleria mellonella* larvae. *FEMS Immunology & Medical Microbiology* 34, 153-157.
- Brothers, K.M., Zachary R. Newman, and Robert T. Wheeler (2011). Live imaging of disseminated candidiasis in zebrafish reveals role of phagocyte oxidase in limiting filamentous growth. *Eukaryotic Cell* 10, 932-944.

Butler, G., Rasmussen, M.D., Lin, M.F., Santos, M.A., Sakthikumar, S., Munro, C.A., Rheinbay, E., Grabherr, M., Forche, A., and Reedy, J.L. (2009). Evolution of pathogenicity and sexual reproduction in eight *Candida* genomes. *Nature* *459*, 657-662.

Chamilos, G., Michail S. Lionakis, Russell E. Lewis, Jose L. Lopez-Ribot, Stephen P. Saville, Nathaniel D. Albert, Georg Halder, and Dimitrios P. Kontoyiannis (2006). *Drosophila melanogaster* as a facile model for large-scale studies of virulence mechanisms and antifungal drug efficacy in *Candida* species. *Journal of Infectious Diseases* *193*, 1014-1022.

Chandra, J., Duncan M. Kuhn, Pranab K. Mukherjee, Lois L. Hoyer, Thomas McCormick, and Mahmoud A. Ghannoum (2001). Biofilm formation by the fungal pathogen *Candida albicans*: development, architecture, and drug resistance. *Journal of Bacteriology* *183*, 5385-5394.

Chávez, V., Mohri-Shiomi, A., Maadani, A., Vega, L.A., and Garsin, D.A. (2007). Oxidative stress enzymes are required for DAF-16-mediated immunity due to generation of reactive oxygen species by *Caenorhabditis elegans*. *Genetics* *176*, 1567-1577.

Conti, H.R., Fang Shen, Namrata Nayyar, Eileen Stocum, Jianing N. Sun, Matthew J. Lindemann, Allen W. Ho et al (2009). Th17 cells and IL-17 receptor signaling are essential for mucosal host defense against oral candidiasis. *The Journal of Experimental Medicine* *206*, 299-311.

Control, C.f.D. (2013). "Fluconazole-Resistant *Candida*". *Antibiotic Resistance Threats in the United States*, 2013, 63.

D'Souza, C.A., Alspaugh, J.A., Yue, C., Harashima, T., Cox, G.M., Perfect, J.R., and Heitman, J. (2001). Cyclic AMP-dependent protein kinase controls virulence of the fungal pathogen *Cryptococcus neoformans*. *Molecular and Cellular Biology* *21*, 3179-3191.

Dieterich, C., Schandar, M., Noll, M., Johannes, F.-J., Brunner, H., Graeve, T., and Rupp, S. (2002). In vitro reconstructed human epithelia reveal contributions of *Candida albicans* EFG1 and CPH1 to adhesion and invasion. *Microbiology* *148*, 497-506.

Douglas, L.J. (2003). *Candida* biofilms and their role in infection. *Trends in microbiology* *11*, 30-36.

Ewbank, J.J. (2002). Tackling both sides of the host-pathogen equation with *Caenorhabditis elegans*. *Microbes and Infection* *4*, 247-256.

Fazly, A., Jain, C., Dehner, A.C., Issi, L., Lilly, E.A., Ali, A., Cao, H., Fidel, P.L., Rao, R.P., and Kaufman, P.D. (2013). Chemical screening identifies filastatin, a small molecule inhibitor of *Candida albicans* adhesion, morphogenesis, and pathogenesis. *Proceedings of the National Academy of Sciences* *110*, 13594-13599.

- Fidel, P.L., Jessica L. Cutright, Larry Tait, and Jack D. Sobel (1996). A murine model of *Candida glabrata* vaginitis. *Journal of Infectious Diseases* 173, 425-431.
- Fidel, P.L., Jose A. Vazquez, and Jack D. Sobel (1999). *Candida glabrata*: review of epidemiology, pathogenesis, and clinical disease with comparison to *C. albicans*. *Clinical Microbiology Reviews* 12, 80-96.
- Filler, S.G., and Sheppard, D.C. (2006). Fungal invasion of normally non-phagocytic host cells. *PLoS pathogens* 2, e129.
- Fraser, J.A., Steven S. Giles, Emily C. Wenink, Scarlett G. Geunes-Boyer, Jo Rae Wright, Stephanie Diezmann, Andria Allen et al (2005). Same-sex mating and the origin of the Vancouver Island *Cryptococcus gattii* outbreak. *Nature* 437, 1360-1364.
- Frohner, I.E., Bourgeois, C., Yatsyk, K., Majer, O., and Kuchler, K. (2009). *Candida albicans* cell surface superoxide dismutases degrade host - derived reactive oxygen species to escape innate immune surveillance. *Molecular microbiology* 71, 240-252.
- Garsin, D.A., Villanueva, J.M., Begun, J., Kim, D.H., Sifri, C.D., Calderwood, S.B., Ruvkun, G., and Ausubel, F.M. (2003). Long-lived *C. elegans* daf-2 mutants are resistant to bacterial pathogens. *Science* 300, 1921-1921.
- Glittenberg, M.T., Ilias Kounatidis, David Christensen, Magali Kostov, Sandra Kimber, Ian Roberts, and Petros Ligoxygakis (2011). Pathogen and host factors are needed to provoke a systemic host response to gastrointestinal infection of *Drosophila* larvae by *Candida albicans*. *Disease models & mechanisms* 4, 515-525.
- Harriott, M.M., Lilly, E.A., Rodriguez, T.E., Fidel, P.L., and Noverr, M.C. (2010). *Candida albicans* forms biofilms on the vaginal mucosa. *Microbiology* 156, 3635-3644.
- Hedayati, M.T., A. C. Pasqualotto, P. A. Warn, P. Bowyer, and D. W. Denning (2007). *Aspergillus flavus*: human pathogen, allergen and mycotoxin producer. *Microbiology* 153, 1677-1692.
- Hodgkin, J., Patricia E. Kuwabara, and Brit Corneliussen. (2000). A novel bacterial pathogen, *Microbacterium nematophilum*, induces morphological change in the nematode *C. elegans*. *Current Biology* 10, 1615-1618.
- Hogan, D.A., Vik, Å., and Kolter, R. (2004). A *Pseudomonas aeruginosa* quorum - sensing molecule influences *Candida albicans* morphology. *Molecular microbiology* 54, 1212-1223.
- Homann, O.R., Jeanselle Dea, Suzanne M. Noble, and Alexander D. Johnson (2009). A phenotypic profile of the *Candida albicans* regulatory network. *PloS genetics* 5, e1000783.

Hong, E., Dixit, S., Fidel, P.L., Bradford, J., and Fischer, G. (2014). Vulvovaginal candidiasis as a chronic disease: diagnostic criteria and definition. *Journal of lower genital tract disease* *18*, 31-38.

Hsu, P.-C., Yang, C.-Y., and Lan, C.-Y. (2011). *Candida albicans* Hap43 is a repressor induced under low-iron conditions and is essential for iron-responsive transcriptional regulation and virulence. *Eukaryotic cell* *10*, 207-225.

Ikeda, F., Yoshimi Wakai, Satoru Matsumoto, Katsuyuki Maki, Etsuko Watabe, Shuichi Tawara, Toshio Goto, Yuji Watanabe, Fumio Matsumoto, and Shogo Kuwahara (2000). Efficacy of FK463, a new lipopeptide antifungal agent, in mouse models of disseminated candidiasis and aspergillosis. *Antimicrobial Agents and Chemotherapy* *44*, 614-618.

Jain, C., Kelly Pastor, Arely Y. Gonzalez, Michael C. Lorenz, and Reeta P. Rao (2013). The role of *Candida albicans* AP-1 protein against host derived ROS in in vivo models of infection. *Virulence* *4*, 67-76.

Jain, C., Yun, M., Politz, S.M., and Rao, R.P. (2009). A pathogenesis assay using *Saccharomyces cerevisiae* and *Caenorhabditis elegans* reveals novel roles for yeast AP-1, Yap1, and host dual oxidase BLI-3 in fungal pathogenesis. *Eukaryotic cell* *8*, 1218-1227.

Joseph Heitman, S.G.F., John E. Edwards, and Aaron P. Mitchell (2006a). *Molecular Principles of Fungal Pathogenesis* (Washington, DC: American Society for Microbiology).

Joseph Heitman, S.G.F., John E. Edwards, and Aaron P. Mitchell (2006b). *Molecular Principles of Fungal Pathogenesis* (Washington, DC: American Society of Microbiology).

Jr, P.L.F. (2002). Distinct protective host defenses against oral and vaginal candidiasis. *Medical Mycology* *40*, 359-375.

Kim, D.H., and Rossi, J.J. (2008). RNAi mechanisms and applications. *Biotechniques* *44*, 613.

Koh, A.Y., Köhler, J.R., Coggshall, K.T., Van Rooijen, N., and Pier, G.B. (2008). Mucosal damage and neutropenia are required for *Candida albicans* dissemination. *Plos pathogens* *4*, e35.

Kornberg, T.B., and Krasnow, M.A. (2000). The *Drosophila* genome sequence: implications for biology and medicine. *Science* *287*, 2218-2220.

Kornitzer, D. (2009). Fungal mechanisms for host iron acquisition. *Current opinion in microbiology* *12*, 377-383.

- Kronstad, J.W., Cadieux, B., and Jung, W.H. (2013). Pathogenic yeasts deploy cell surface receptors to acquire iron in vertebrate hosts. *PLoS pathogens* 9, e1003498.
- Kumamoto, C.A., and Vinces, M.D. (2005a). Alternative *Candida albicans* lifestyles: growth on surfaces. *Annu Rev Microbiol* 59, 113-133.
- Kumamoto, C.A., and Vinces, M.D. (2005b). Contributions of hyphae and hypha - co - regulated genes to *Candida albicans* virulence. *Cellular microbiology* 7, 1546-1554.
- Leclerc, V., and Reichhart, J.M. (2004). The immune response of *Drosophila melanogaster*. *Immunological reviews* 198, 59-71.
- Lemaitre, B., Nicolas, E., Michaut, L., Reichhart, J.-M., and Hoffmann, J.A. (1996). The Dorsoventral Regulatory Gene Cassette *spätzle/Toll/cactus* Controls the Potent Antifungal Response in *Drosophila* Adults. *Cell* 86, 973-983.
- Lewis, L.E., Bain, J.M., Lowes, C., Gillespie, C., Rudkin, F.M., Gow, N.A., and Erwig, L.-P. (2012). Stage specific assessment of *Candida albicans* phagocytosis by macrophages identifies cell wall composition and morphogenesis as key determinants. *PLoS pathogens* 8, e1002578.
- Lewis, L.E., Bain, J.M., Okai, B., Gow, N.A., and Erwig, L.P. (2013). Live-cell video microscopy of fungal pathogen phagocytosis. *Journal of visualized experiments: JoVE*.
- Li, Y., Ma, Y., Zhang, L., Guo, F., Ren, L., Yang, R., Li, Y., and Lou, H. (2012). In vivo inhibitory effect on the biofilm formation of *Candida albicans* by liverwort derived riccardin D. *PloS one* 7, e35543.
- Liu, H., Kohler, J., and Fink, G.R. (1994). Suppression of hyphal formation in *Candida albicans* by mutation of a STE12 homolog. *Science* 266, 1723-1726.
- Lo, H.-J., Julia R. Köhler, Beth DiDomenico, David Loebenberg, Anthony Cacciapuoti, and Gerald R. Fink (1997). Nonfilamentous *C. albicans* mutants are avirulent. *Cell* 90, 939-949.
- Lo, H.-J., Köhler, J.R., DiDomenico, B., Loebenberg, D., Cacciapuoti, A., and Fink, G.R. (1997). Nonfilamentous *C. albicans* mutants are avirulent. *Cell* 90, 939-949.
- Lopez-Berestein, G., Hopfer, R., Mehta, R., Mehta, K., Hersh, E., and Juliano, R. (1984). Liposome-encapsulated amphotericin B for treatment of disseminated candidiasis in neutropenic mice. *Journal of Infectious Diseases* 150, 278-283.
- Lorenz, M.C., Bender, J.A., and Fink, G.R. (2004). Transcriptional response of *Candida albicans* upon internalization by macrophages. *Eukaryotic Cell* 3, 1076-1087.

Lorenz, M.C., and Fink, G.R. (2001). The glyoxylate cycle is required for fungal virulence. *Nature* 412, 83-86.

Mahajan-Miklos, S., Man-Wah Tan, Laurence G. Rahme, and Frederick M. Ausube (1999). Molecular Mechanisms of Bacterial Virulence Elucidated Using a *Pseudomonas aeruginosa*–*Caenorhabditis elegans* Pathogenesis Model. *Cell* 96, 47-56.

Mayer, F.L., Wilson, D., and Hube, B. (2013). *Candida albicans* pathogenicity mechanisms. *Virulence* 4, 119-128.

McRipley, R., Erhard, P., Schwind, R., and Whitney, R. (1979). Evaluation of vaginal antifungal formulations in vivo. *Postgraduate medical journal* 55, 648-652.

Mylonakis, E., Frederick M. Ausubel, John R. Perfect, Joseph Heitman, and Stephen B. Calderwood (2002). Killing of *Caenorhabditis elegans* by *Cryptococcus neoformans* as a model of yeast pathogenesis. *Proceedings of the National Academy of Sciences* 99, 15675-15680.

Mylonakis, E., Idnurm, A., Moreno, R., El Khoury, J., Rottman, J.B., Ausubel, F.M., Heitman, J., and Calderwood, S.B. (2004). *Cryptococcus neoformans* Kin1 protein kinase homologue, identified through a *Caenorhabditis elegans* screen, promotes virulence in mammals. *Molecular microbiology* 54, 407-419.

Németh, T., Adél Tóth, Judit Szenzenstein, Péter Horváth, Joshua D. Nosanchuk, Zsuzsanna Grózer, Renáta Tóth et al (2013). Characterization of Virulence Properties in the *C. parapsilosis* Sensu Lato Species. *PLoS ONE* 8, e68704.

Noble, S.M. (2013). *Candida albicans* specializations for iron homeostasis: from commensalism to virulence. *Current opinion in microbiology* 16, 708-715.

Noble, S.M., French, S., Kohn, L.A., Chen, V., and Johnson, A.D. (2010). Systematic screens of a *Candida albicans* homozygous deletion library decouple morphogenetic switching and pathogenicity. *Nature genetics* 42, 590-598.

O'Toole, G., Kaplan, H.B., and Kolter, R. (2000). Biofilm formation as microbial development. *Annual Reviews in Microbiology* 54, 49-79.

Pendrak, M.L., Chao, M.P., Yan, S.S., and Roberts, D.D. (2004). Heme oxygenase in *Candida albicans* is regulated by hemoglobin and is necessary for metabolism of exogenous heme and hemoglobin to α -biliverdin. *Journal of Biological Chemistry* 279, 3426-3433.

Pfaller, M.A., and D. J. Diekema (2007). Epidemiology of invasive candidiasis: a persistent public health problem. *Clinical Microbiology Reviews* 20, 133-163.

Prevention, C.f.D.C.a. (2014a). *C. neoformans* cryptococcosis.

Prevention, C.f.D.C.a. (2014b). Candidiasis.

Prevention, C.f.D.C.a. (2014c). Fungal Disease.

Prevention, C.f.D.C.a. (2014d). Histoplasmosis.

Price, M.S., Marisol Betancourt-Quiroz, Jennifer L. Price, Dena L. Toffaletti, Haily Vora, Guanggan Hu, James W. Kronstad, and John R. Perfect (2011). *Cryptococcus neoformans* requires a functional glycolytic pathway for disease but not persistence in the host. *MBio* 2.

Pukkila-Worley, R., Ausubel, F.M., and Mylonakis, E. (2011). *Candida albicans* infection of *Caenorhabditis elegans* induces antifungal immune defenses. *PLoS pathogens* 7, e1002074.

Quintin, J., Asmar, J., Matskevich, A.A., Lafarge, M.-C., and Ferrandon, D. (2013). The *Drosophila* Toll pathway controls but does not clear *Candida glabrata* infections. *The Journal of Immunology* 190, 2818-2827.

Ramage, G., Saville, S.P., Thomas, D.P., and López-Ribot, J.L. (2005). *Candida* biofilms: an update. *Eukaryotic cell* 4, 633-638.

Rao, R. (2015a). The Hypothesis for the Second Screen. In Adobe Illustrator.

Rao, R. (2015b). Iron-Uptake Pathway Working within the Cell. In Adobe Illustrator.

Rao, R. (2015c). The Original Hypothesis for the Initial Screen. In Adobe Illustrator.

Rao, R.P., Hunter, A., Kashpur, O., and Normanly, J. (2010). Aberrant synthesis of indole-3-acetic acid in *Saccharomyces cerevisiae* triggers morphogenic transition, a virulence trait of pathogenic fungi. *Genetics* 185, 211-220.

Rappleye, C.A., Jacquelyn T. Engle, and William E. Goldman (2004). RNA interference in *Histoplasma capsulatum* demonstrates a role for α - (1, 3) - glucan in virulence. *Molecular microbiology* 53, 153-165.

Robbins, S.L., Kumar, V., and Cotran, R.S. (2010). Robbins and Cotran pathologic basis of disease, 8th edn (Philadelphia, PA: Saunders/Elsevier).

Rosch, R.N.a.J. (2015). Testing the Effectiveness of Filastatin using Atomic Force Microscopy (Major Qualifying Project Worcester Polytechnic Institute).

Rubin-Bejerano, I., Fraser, I., Grisafi, P., and Fink, G.R. (2003). Phagocytosis by neutrophils induces an amino acid deprivation response in *Saccharomyces cerevisiae* and *Candida albicans*. *Proceedings of the National Academy of Sciences* *100*, 11007-11012.

Schaller, M., Matthias Bein, Hans C. Korting, Stefan Baur, Gerald Hamm, Michel Monod, Sabine Beinhauer, and Bernhard Hube (2003). The secreted aspartyl proteinases Sap1 and Sap2 cause tissue damage in an in vitro model of vaginal candidiasis based on reconstituted human vaginal epithelium. *Infection and Immunity* *71*, 3227-3234.

Sehgal, S., Baker, H., and Vézina, C. (1975). Rapamycin (AY-22,989), a new antifungal antibiotic. II. Fermentation, isolation and characterization. *The Journal of antibiotics* *28*, 727-732.

Selmecki, A., Forche, A., and Berman, J. (2010). Genomic plasticity of the human fungal pathogen *Candida albicans*. *Eukaryotic cell* *9*, 991-1008.

Shea, A., Wolcott, M., Daefler, S., and Rozak, D.A. (2012). Biolog phenotype microarrays. In *Microbial Systems Biology* (Springer), pp. 331-373.

Sheftel, A.D., Mason, A.B., and Ponka, P. (2012). The long history of iron in the Universe and in health and disease. *Biochimica et Biophysica Acta (BBA)-General Subjects* *1820*, 161-187.

Sheikh, N., Jahagirdar, V., Kothadia, S., and Nagoba, B. (2013). Antifungal drug resistance in *Candida* species. *Eur J Gen Med* *10*, 254-258.

Sherman, F. (1991). Getting started with yeast. *Methods Enzymol* *194*, 21.

Stiernagle, T. (2006). Maintenance of *C. elegans*. *WormBook*. The *C. elegans* Research Community. *WormBook*.

Summerton, J., and WELLER, D. (1997). Morpholino antisense oligomers: design, preparation, and properties. *Antisense and Nucleic Acid Drug Development* *7*, 187-195.

Taff, H.T., Nett, J.E., Zarnowski, R., Ross, K.M., Sanchez, H., Cain, M.T., Hamaker, J., Mitchell, A.P., and Andes, D.R. (2012). A *Candida* biofilm-induced pathway for matrix glucan delivery: implications for drug resistance. *PLoS pathogens* *8*, e1002848.

Takakura, N., Yuichi Sato, Hiroko Ishibashi, Haruyuki Oshima, Katsuhisa Uchida, Hideyo Yamaguchi, and Shigeru Abe (2003). A novel murine model of oral candidiasis with local symptoms characteristic of oral thrush. *Microbiology and Immunology* *47*, 321-326.

Thewes, S., Marianne Kretschmar, Hyunsook Park, Martin Schaller, Scott G. Filler, and Bernhard Hube (2007). In vivo and ex vivo comparative transcriptional profiling of invasive

and non - invasive *Candida albicans* isolates identifies genes associated with tissue invasion. *Molecular microbiology* 63, 1606-1628.

Tobin, D.M., Robin C. May, and Robert T. Wheeler (2012). Zebrafish: A see-through host and a fluorescent toolbox to probe host–pathogen interaction. *PLoS pathogens* 8, e1002349.

van der Sar, A.M., Appelmelk, B.J., Vandenbroucke-Grauls, C.M., and Bitter, W. (2004). A star with stripes: zebrafish as an infection model. *Trends in microbiology* 12, 451-457.

Weissman, Z., and Kornitzer, D. (2004). A family of *Candida* cell surface haem - binding proteins involved in haemin and haemoglobin - iron utilization. *Molecular microbiology* 53, 1209-1220.

Wheeler, R.T., and Fink, G.R. (2006). A drug-sensitive genetic network masks fungi from the immune system. *PLoS pathogens* 2, e35.

Willger, S.D., Srisombat Puttikamonkul, Kwang-Hyung Kim, James B. Burritt, Nora Grahl, Laurel J. Metzler, Robert Barbuch, Martin Bard, Christopher B. Lawrence, and Robert A. Cramer Jr. (2008). A sterol-regulatory element binding protein is required for cell polarity, hypoxia adaptation, azole drug resistance, and virulence in *Aspergillus fumigatus*. *PLoS pathogens* 4.

Wormley, F.L., Chad Steele, Karen Wozniak, Kohtaro Fujihashi, Jerry R. McGhee, and Paul L. Fidel (2001). Resistance of T-cell receptor δ -chain-deficient mice to experimental *Candida albicans* vaginitis. *Infection and Immunity* 69, 7162-7164.

Xu, N., Qian, K., Dong, Y., Chen, Y., Yu, Q., Zhang, B., Xing, L., and Li, M. (2014). Novel role of the *Candida albicans* ferric reductase gene CFL1 in iron acquisition, oxidative stress tolerance, morphogenesis and virulence. *Research in microbiology* 165, 252-261.